ENCAPSULATION OF ROLLING CIRCLE AMPLIFICATION PRODUCT IN HYDROGEL SYSTEMS FOR APPLICATIONS IN BIOSENSING

By SOPHIA EMERSON, B. Eng. Biosci.

A Thesis Submitted to the School of Graduate Studies in Partial Fulfillment of the Requirements for the Degree of Master of Applied Science

McMaster University MASTER OF APPLIED SCIENCE (2019) Hamilton, Ontario (Chemical Engineering)

TITLE: Encapsulation of rolling circle amplification product in hydrogel systems for applications in biosensing

AUTHOR: Sophia Emerson, B.Eng. Biosci. (McMaster University)

SUPERVISORS: Dr. Carlos Filipe and Dr. Todd Hoare

NUMBER of PAGES: xii, 71

Abstract

The development of easily fabricated, highly stable DNA-based microarray and continuous flow concentrating devices is vital for several biomedical and environmental applications. Nucleic acid biosensors can be used for genetic analysis, disease diagnosis, drug discovery, food and water quality control and more, however methods of fabrication are tedious, and the longevity of sensors is compromised by the fragility of the sensing component. In this report, the fabrication and characterization of two biosensing modalities – microarrays and microgels – composed of Rolling Circle Amplification (RCA) product in poly(oligoethylene glycol methacrylate) (POEGMA) hydrogels are investigated. RCA product microarrays were developed by the sequential printing of aldehyde and hydrazide functionalized POEGMA precursors on nitrocellulose paper, exploiting rapid gelling via hydrazone crosslinking to generate thin film hydrogel sensing arrays. POEGMA/RCA product microgels for affinity column applications were synthesized using an inverse emulsion polymerization technique. Inkjet printing evenly deposited RCA product in all wells, with POEGMA effectively stabilizing DNA on the cellulose substrate. Hybridization of complementary probe to the encapsulated RCA product was optimized, yielding a signal to noise ratio of ~4 for a large range of probe concentrations. Microgels were successfully synthesized in the size range of 10-60 μm diameter, and a linear model that can accurately predict size based on initiator and emulsifier concentration was developed. The encapsulation efficiency of RCA product in different sized microgels was explored, with larger microgels entrapping more product and the highest encapsulation efficiency calculated at 56%. These results demonstrate that POEGMA hydrogels can be utilized to encapsulate and stabilize RCA product in two distinct structures, providing a basis for the development of easily fabricated biosensors for more specific applications.

Acknowledgements

First and foremost, I would like to thank my supervisors Dr. Todd Hoare and Dr. Carlos Filipe for their continued guidance and encouragement over the course of my M.A.Sc. research. Todd, thank you for having a solution or suggestion upon every wall I hit, your recommendations kept me on track and directed me towards an end product that I am exceptionally proud of. Carlos, your unwavering belief in me from the moment I started working in your lab in 2015 is astounding. I do not think I would be where I am today without having you in my corner, and I am forever grateful for your support.

I am incredibly appreciative of the hard work of my undergraduate research assistants, Mariam Sidawi, Matana Hendrickson, and Cherrie Hung. Not only did your efforts help my experiments come together so quickly, but your presence in the lab made long summer hours of research incredibly joyful; full of laughs and ice-cream breaks.

I would like to acknowledge several members of the Hoare lab for their advice and technical assistance. To Dr. Rabia Mateen, Milana Pikula, and Madeline Simpson, thank you for guiding me on polymer synthesis and Biojet printing when this project was still in its infancy. To Ali Babar, Matthew Campea, and Michael Kiriakou, thank you for sharing your triumphs and failures in the tedious and finicky world of emulsion science, our frequent brainstorming sessions were extremely valuable.

I would also like to thank Dr. Vincent Leung for serving as a long-time mentor, colleague, and friend. Your constant advice throughout the duration of my work gave me the perspective necessary to complete this thesis despite the many bumps that accompany academic research.

I am endlessly thankful for the loving encouragement from my parents, who've stood behind every dream I've chased and always inspired me to work hard. Last but certainly not least, thank you to my dear friend Alexandre D'Souza, for both technical and emotional support in this journey. Diamonds sure are made under pressure, and our friendship is a testament to that.

Table of Contents

List of Figures and Tables

List of Abbreviations and Symbols

AA: Acrylic acid

ADH: Adipic acid dihydrazide

AIBMe: 2,2-azobisisobutryic acid dimethyl ester

AIBN: azo-bis-isobutyronitrile

APS: Ammonium persulfate

BSA: Bovine serum albumin

CT: Circular template

DIW: Deionized water

DMAEMA: N,N-dimethylaminoethyl methacrylate

DMEMAm: N-(2,2-dimethoxyethyl)methacrylamide

dNTP: Deoxyribonucleotide triphosphates

DOE: Design of Experiments

dPAGE: denatured polyacrylamide gel electrophoresis

EDC: N'-ethyl-N-(3-dimethylaminopropyl)-carbodiimide

EGDMA: Ethylene glycol dimethacrylate

FP: Fluorescein-labeled probe

HCL: Hydrochloric acid

HLB: Hydrophilic-Lipophilic Balance

LT: Ligation template

OEGMA: Oligo(ethylene glycol) methyl ether methacrylate

PBS: Phosphate buffered saline

PEG: Polyethylene glycol

PNK: Polynucleotide kinase

POA: Aldehyde functionalized poly(oligoethylene glycol methacrylate)

POEGMA: poly(oligoethylene glycol methacrylate)

POH: Hydrazide functionalized poly(oligoethylene glycol methacrylate)

RCA: Rolling Circle Amplification

s.d: Standard deviation

SDS: Sodium dodecyl sulfate

SELEX: systematic evolution of ligands by exponential enrichment

SSC: Saline-sodium citrate

Tm: Melting temperature

VPTT: Volume Phase Transition Temperature

Declaration of Academic Achievement

The majority of the work presented in this thesis was developed, executed, analyzed, and written by the author in consultation with Dr. Carlos Filipe and Dr. Todd Hoare, except for the following:

Chapter 3: several microgel images were captured and analyzed with the assistance of my undergraduate students, Mariam Sidawi and Cherrie Hung.

Chapter 1: Motivation and Research Objectives

1.1 Biochemical-based detection systems

Biological systems have evolved elegant structures for recognition of and pairing to highly specific molecular targets. Enzyme-substrate interactions, antibody-antigen pairing, and annealing of complementary nucleic acid sequences are all examples of precise biochemical interactions.[1] Such interactions have been exploited in biosensor technology, wherein a biological element – or biomimetic component – is utilized to interact or bind with a chemical entity, and a transducer transforms the signal into a quantifiable one.[2] Different combinations of detection systems and transduction methods exist to quantify or monitor a vast range of analytes, making the applications of biosensor technology nearly endless. These recognition elements have been utilized in point-of-care devices such as glucose monitors[3] and pregnancy tests[4], for environmental monitoring including the detection of heavy metals[5] and pesticides[6] in river systems, and even in food and water quality control (e.g. detection of residual antibiotics in meat[7]).

Nucleic acids are of particular interest as the biological component in biosensors due in part to the explosion of detection schemes that followed the discovery of aptamers.[8] DNA aptamers are short oligonucleotide sequences that are artificially evolved to detect a particular target via several rounds of in vitro selection for a highly specific folded structure.[9, 10] With aptamers, nucleic acids have the capacity to bind to a range of targets beyond their complementary sequence, opening up the applications for DNA-based detection systems.

1.1.1 Nucleic acid recognition events

Nucleic acids can recognize their own complementary targets or highly specific chemical analytes due sequences that lend themselves to particularly folded shapes. Sequence-specific

recognition results from Watson-Crick base pairing (adenine with thymine and cytosine with guanine), whereby single stranded DNA hybridizes to a complementary sequence to create a duplex stabilized by hydrogen bonding, depicted in Figure 1.1 (a). The double stranded molecule will be stable in temperatures below the melting temperature (T_m), which is dictated by the proportion of AT pairs to GC pairs in the sequence.[11] Separation of hybridized sequences can be achieved by raising the temperature above the T_m, by increasing the pH such that additional hydroxide ions disrupt hydrogen bonding, or by lowering the ionic strength of the solution.[11]

Nucleic acid aptamers are generated by systematic evolution of ligands by exponential enrichment (SELEX) to advance towards a sequence that will preferentially fold or self-anneal to form precise structures.[10] Aptamers bind to targets much like enzymes bind to substrates in a "lock and key" model, in which the complementary shapes of the aptamer and the target coupled with electrostatic and hydrophobic interactions stabilize the aptamer-target pair (Figure 1.1 (b)).

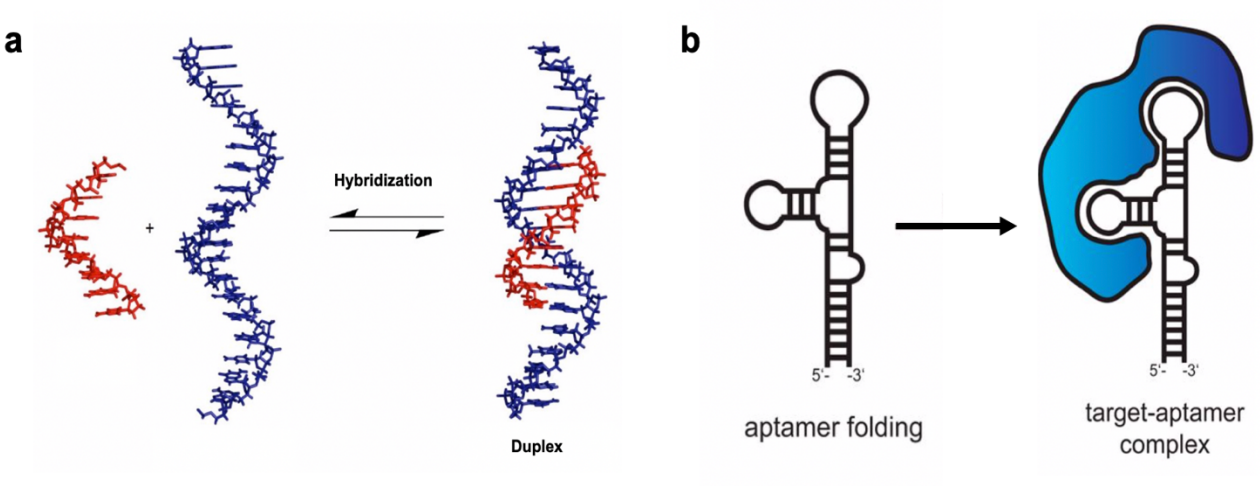

Figure 2.1 Different nucleic acid recognition events. **(a)** hybridization of complementary DNA strands, reproduced from Minuth.[12] **(b)** Binding between a functional aptamer and its target, adapted from Wolter and Mayer.[13]

1.1.2 DNA microarrays

One prominent use of DNA-based detection lies in DNA microarrays, which employ complementary hybridization events for rapid, multiplex analysis of nucleic acids.[14] Microarrays typically consist of thousands of small reaction zones containing different DNA probes for a library of targets immobilized on a solid support.[14] Probes are usually short sequences that can hybridize to complementary DNA targets, allowing for rapid, parallelized detection of different DNA sequences. With their ability of analyzing multiple sequences simultaneously, microarray technology has found its merit in streamlining the diagnosis of genetic diseases[15], measurements of gene expression[16], analysis of forensic evidence[17], drug development[18], and more.

DNA microarrays conventionally consist of two-dimensional collections of biomolecules attached to glass, plastic, or silicon chips.[19] Proper immobilization of DNA is vital for the success of the array; probes must be oriented properly and at a high enough density in order to be accessible to the target and sensitive enough for the detection of low signals.[19] Moreover, probes must be firmly affixed in a highly uniform manner, as any loss of probe or uneven deposition would limit the conclusions that can be drawn from zone-to-zone comparisons.[20] This particularly important when microarrays are utilized in the *quantification* of nucleic acid expression as opposed to simply detecting the presence or absence of a particular DNA sequence.

Well-established methods of attaching DNA to surfaces include covalent bonding to the support (e.g. acid treatment of glass to expose hydroxyl groups for linkage to phosphate residues on DNA[21]), thiolated DNA for chemisorption onto gold substrates[22], use of biotinylated DNA for complexation with surface-immobilized streptavidin[23], and simple adsorption onto carbon structures.[24] Unfortunately, automation of microarray production (typically performed via photolithography or contact/non-contact printing[25]) is limited by the complex nature of several of

the discussed immobilization strategies. Furthermore, the density of the reporter oligonucleotides can only be pushed so far; a critical threshold exists wherein a steric hindrance to hybridization ensues due to the high probe density.[26] Exposed DNA is also vulnerable to degradation by environmental stresses such as mechanical shearing or nuclease activity, reducing the stability and lifetime of such arrays. Hybridization of targets to reporter oligos poses an additional issue, as interfacial hybridization events demonstrate slow kinetics relative to solution based assays.[27] As such, although DNA microarrays are well-established as a sensing platform, there are clearly still many challenges to be addressed for the improvement of DNA microarray technologies.

1.1.3 DNA-based concentration and detection strategies

There is a high demand for the development of methods for the detection of ultralow levels of chemical markers. Improving detection limits is of interest for the early diagnosis and monitoring of clinical disorders such as cancer and heart disease. Moreover, clinical samples typically require DNA isolation and concentration steps via silica monoliths prior to analysis; however, the recovery rates of DNA using such methods are quite low and the strategy employed is non-specific, resulting in the isolation of all DNA from a mixture regardless of its sequence.[28] Beyond microarray applications, DNA recognition events can also be utilized as a basis for highly specific target capture and concentration.

Several ultra-low DNA-based sensors for particular analytes have been reported, each incredibly unique in their approach. For example, Liu et al. developed a method for detecting prostate-specific antigen at concentrations as low as 0.032 pg/mL via activatable fluorescence of Rhodamine B isothiocyanate conjugated to fluorescence quenching gold nanoparticles.[29] Umar et al. have demonstrated highly sensitive cholesterol biosensors composed of cholesterol oxidase physically adsorbed onto zinc oxide nanoparticles coated onto a gold electrode for amperometric

biosensing.[30] One common motif is the covalent linkage of specific gene sequences or aptamers for particular targets to microstructure supports.[31-33] Functionalized particles can then be packed into columns to create a continuous flow biosensor wherein targets are concentrated in the column and then eluted with a change in salt induced by elution buffer, enabling further analysis. The general process is similar to DNA isolation via commercially established silica columns; however, the advantage lies in the ability to separate a *specific* gene as opposed to all DNA present in a sample. Unfortunately, covalent linkage to a solid microparticle support maintains the same drawbacks as discussed in section 1.1.2, namely a lack of stability against nucleases or shearing and the complicated chemistry involved with fabrication. There remains a need for a simple and stable DNA-based concentration platform, amendable to a variety of target molecules without significant adjustments to manufacturing techniques.

1.2 Hydrogel systems

Hydrogels are three dimensional networks of crosslinked hydrophilic polymers that can swell in water while maintaining a desired structure.[34] Due to their chemical and mechanical similarity to human tissue, hydrogels have long been employed in biomedical applications such as tissue regeneration and drug delivery.[35] The properties of hydrogels have also made them attractive in DNA-based biosensing applications, mitigating many of the challenges discussed in section 1.1.[36] With their three-dimensional structure, hydrogels enhance the capacity for reporter oligo encapsulation beyond the limits of 2D structures.[37] Polymer chains can also present a steric barrier to nuclease enzymes, protecting the sensitive biological element and lengthening the lifetime of the sensor.[38] Moreover, their aqueous internal environment improves the kinetics of hybridization to match or at least approximate those of solution-based hybridization reactions[39], with the highly porous structure of hydrogels allowing for facile diffusion of molecular targets.

Several studies have reported the use of hydrogels for nucleic acid biosensors. Beyer et al. described a hydrogel microarray for DNA analysis by covalently attaching thiol-modified DNA during the polymerization process.[40] Baeissa et al. demonstrated highly sensitive and re-usable sensors for target DNA by covalently functionalizing a polyacrylamide gel with acrydite-modified DNA during polymerization.[41] Aptamer-functionalized microgels for continuous flow biosensors have also been developed, with Srinivas et al. reporting polyethylene glycol hydrogel microparticles linked with an aptamer capture sequence for human α-thrombin.[42] As evident from a review of the literature, covalent binding is the most widely utilized method for DNA incorporation, due mainly to the stability it confers. Physical entrapment of DNA is advantageous as it negates the need for chemical modification of DNA prior to synthesis; however there is potential for leakage of the sensing component.[43] To avoid undesirable loss of the reporter oligo, hydrogel pores must be significantly smaller in size than the bioreceptor.[36] Given that lowering the hydrogel pore size also inhibits the diffusion of target molecules into the gel (thus compromising the kinetics of the detection event), physical incorporation of DNA inside hydrogels is rarely reported.

1.2.1 Poly(oligoethylene glycol methacrylate) hydrogels

In recent years, poly(oligoethylene glycol methacrylate) (POEGMA) hydrogels have emerged as promising systems for a variety of biomedical applications, primarily due to their low cytotoxicity and excellent antifouling properties.[44] POEGMA hydrogels are intriguing due to their tunable chemistry that enables for the production of a vast array of hydrogel systems with different mechanical strengths[45], porosities[46], thermoresponsivities[47], and charge densities[48].

There are a number of different strategies for the polymerization and crosslinking of POEGMA hydrogels. Polymerization typically ensues via a free radical co-polymerization[44], by

which OEGMA monomer can be combined with monomers of different ethylene glycol chain lengths, such as diethylene glycol methacrylate, to create statistical POEGMA copolymers of different hydrophilicities and swelling characteristics.[49]

Crosslinking of POEGMA polymers to form hydrogels can be achieved by physical means (hydrogen bonding, affinity interactions) or chemical strategies. Chemically crosslinked networks are typically preferred due to their stability and/or capacity for highly controlled degradation. Chemical crosslinking can be achieved by including a bifunctional monomer (e.g. ethylene glycol dimethacrylate (EGDMA)) during the polymerization reaction that can link two growing polymer chains. Alternately, functional groups can be grafted to linear polymers that can form crosslinks between the chains when mixed, such as hydrazide or amine groups reacting with aldehyde groups on complementarily-functionalized polymers. Of particular interest, aldehyde-hydrazide functional groups can react together to form hydrazone bonds, advantageous due to their rapid formation, high stability, and reversibility upon changes to the pH. Aldehyde and hydrazide groups can be chemically incorporated into polymer precursors during free radical polymerization by including the comonomers N-(2,2-dimethoxyethyl)methacrylamide (DMEMAm), which is subsequently hydrolyzed post-polymerization to generate aldehyde groups, or acrylic acid, which is subsequently conjugated with adipic acid dihydrazide, during the polymerization process (depicted in Figure 1.2 a and b).[50] The mol% of functional groups can be adjusted by altering the ratio of monomers added, allowing for tight control of the crosslinking density and thus hydrogel pore size. Charge on polymer precursors can also be induced by the copolymerization of N,N-dimethylaminoethyl methacrylate (for cationic precursors) or acrylic acid (for anionic precursors), and the charge density can be controlled by changing the mol% of these monomers (demonstrated in Figure 1.2 c and d).[48]

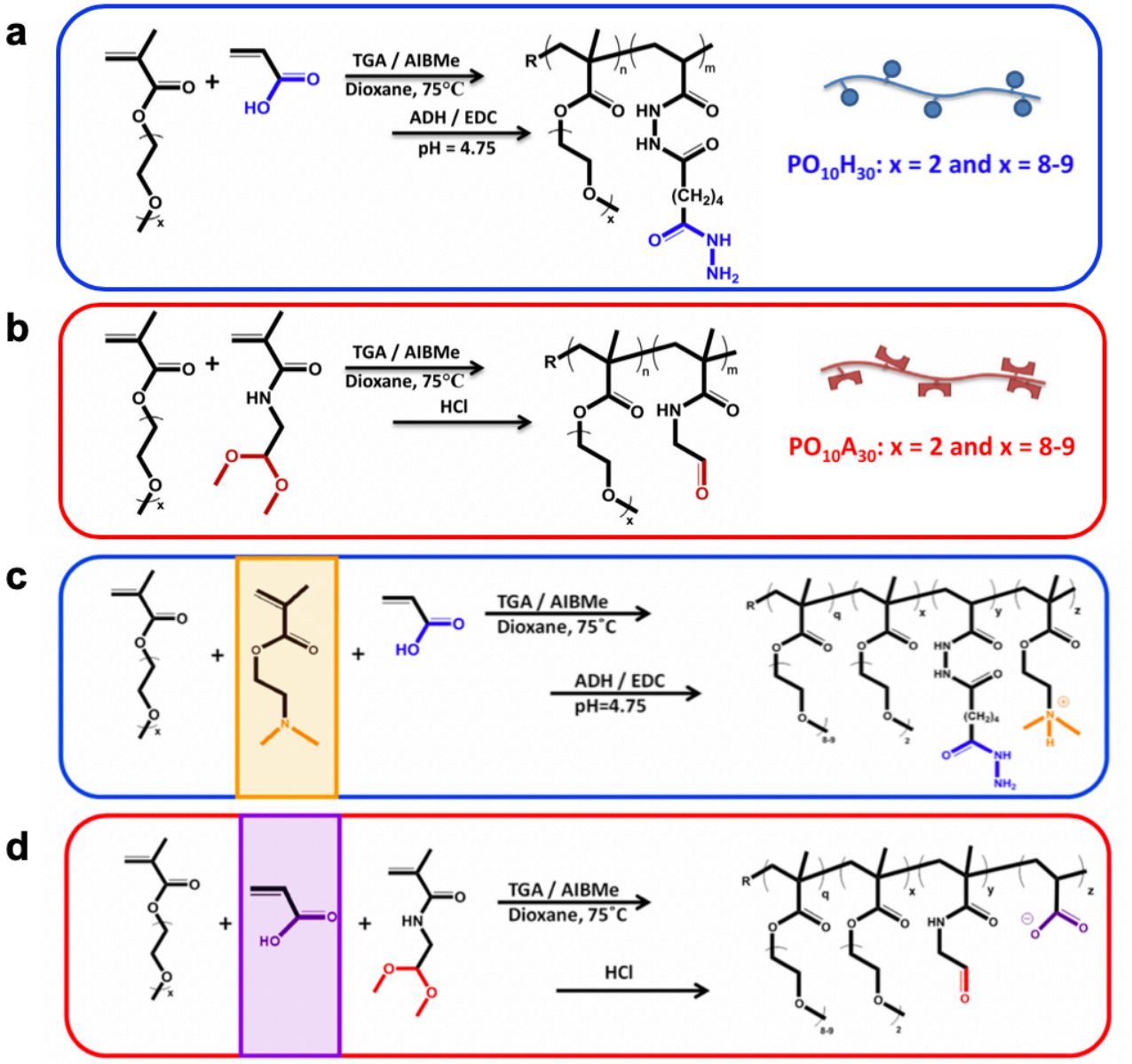

Figure 1.2. Schematic representation of the synthesis of POEGMA precursors; (a) hydrazide functionalized POEGMA (POH) (b) aldehyde functionalized POEGMA (POA) (c) cationic hydrazide functionalized POEGMA and (d) anionic aldehyde functionalized POEGMA, adapted from Smeets et al. and Bakaic et al.[48, 50]

1.2.2 Thin Film POEGMA hydrogels

The macrostructure of POEGMA hydrogels can be controlled by the technique employed during polymerization and crosslinking. Surface attached hydrogel films are advantageous as the smaller dimensions reduce the diffusion time of targets through the gel, making them particularly suited for use in microarray technologies. Thin film POEGMA hydrogels can be produced by depositing small volumes of dilute aldehyde and hydrazide functionalized polymer precursors onto a receptive substrate in a sequential manner. Different methods can be employed to lay down the polymer, including spin coating[51], non-contact printing[52], and dip coating[53]. For instance, Deng et al. demonstrated a paper-based device as a platform for enzyme-linked immunosorbent assay synthesized by sequentially dipping a nitrocellulose substrate in aldehyde functionalized POEGMA followed by hydrazide functionalized POEGMA, generating a thin protein-resistant film on the substrate.[54] For scale-up purposes vital in microarray development, printing is of interest as it can allow for controlled deposition in specific patterns utilizing an automated technology.

1.2.3 Polymerization of POEGMA microgels

POEGMA microgels can be synthesized by altering the polymerization technique such that radical polymerization is confined to small reaction droplets within an immiscible solvent. In inverse emulsion polymerization, droplets of water-soluble monomer (OEGMA) and crosslinker (EGDMA) are dispersed in an oil phase to create a colloidal dispersion stabilized by emulsifiers.[55] Addition of initiator induces free radical polymerization, leading to nano or micro sized particles for oil and water-soluble initiators, respectfully.[56] The choice of the emulsifier depends on the hydrophilic-lipophilic balance (HLB) in the system, with an emulsifier combination of similar HLB to the oil employed typically leading to the most stable emulsion.[57] The size of the polymer

particles can be controlled by adjustments to the emulsifier concentration, initiator concentration, viscosity of the continuous phase, temperature of the reaction, and speed of agitation.[58-61]

Water-in-oil emulsions have been reported for the entrapment of nucleic acids. Tawfik et al. reported the transcription and translation of single genes within aqueous drops (several microns in diameter) dispersed in an oil phase.[62] Similarly, Nakano et al. demonstrated polymerase chain reaction within "microreactors" – dispersed water droplets in a water in oil emulsion.[63] Evidently, DNA preferentially partitions into the water phase of said emulsions due to its hydrophilic sugar-phosphate backbone. This behavior can be exploited to create microgels with entrapped DNA for target concentration and biosensing applications.

1.3 Rolling Circle Amplification product

Rolling Circle Amplification (RCA) is an isothermal replication process utilized to augment a particular gene by rapidly synthesizing multiple copies linked together in a single stranded DNA strand.[64, 65] The technique is typically used for amplifying ultralow DNA amounts for ease of analysis. DNA polymerase adds free deoxyribonucleotide triphosphates (dNTP's) to a short primer annealed to a complementary circle template, as depicted in Figure 1.3.[65] As the polymerase works around the circle, the annealed strand "falls off" of the circle such that thousands of complementary copies of the circle template are synthesized in series. The amplification strategy is akin to a polymerization reaction, in which the sequence complementary to the circle represents monomer, and the resultant tandem DNA strand is a polymeric molecule more specifically referred to as a concatemer.

RCA product can grow to lengths extending over several microns, limited only by the amount of dNTP's in solution and the time at which the reaction is terminated by enzyme denaturation.[66] Due to its length, RCA product can be physically immobilized by hydrogel systems

without having to shrink the gel pore size and hinder target molecule diffusion. The simplicity of incorporation (in comparison to described covalent attachment mechanisms) makes it an attractive molecule as the sensing element in hydrogel/DNA biosensors. Moreover, its repetitive nature – composed of thousands of copies of the same sequence – allows for a high density of reporter oligo thus boosting biosensor sensitivity. RCA product can be incorporated into both hydrogel microarrays or microgels, and it can be used to detect a complementary sequence directly or employed as a single stranded "backbone" for conjugation of aptamers for more specific targets. Thus, physical incorporation of RCA product within hydrogel systems is both an elegant and novel assembly for nucleic acid-based detection or concentration of a wide variety of analytes.

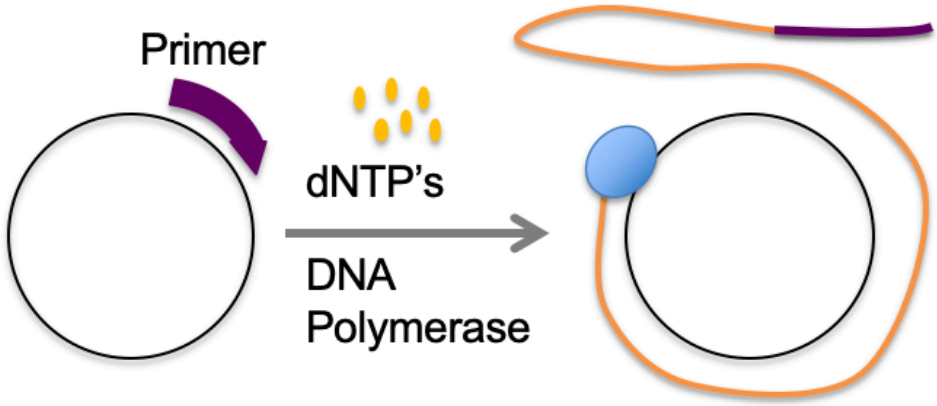

Figure 1.3. Synthesis of Rolling Circle Amplification product.

1.4 Thesis Objectives

The primary goal of this work was to develop and characterize hydrogel systems with physically entrapped RCA product. Different polymerization techniques were employed to generate (1) thin film hydrogels for microarray applications and (2) spherical microgels for continuous flow biosensor development. POEGMA was selected as the polymer of choice due to

its attractive properties in biological applications and the diverse chemistry that can be manipulated to improve RCA product orientation within the hydrogels.

In Chapter 2, printed POEGMA microarrays are developed via subsequent deposition of aldehyde functionalized polymer followed by hydrazide functionalized polymer "inks" equipped with RCA product onto a nitrocellulose substrate (demonstrated in Figure 1.4). The uniformity of RCA product printing was probed to ascertain whether the system would be of value in microarray applications. Furthermore, the ability of the crosslinked POEGMA hydrogel to immobilize the RCA product on the nitrocellulose was investigated. Lastly, the system was probed with oligos complementary to the printed RCA product and the conditions for hybridization were adjusted to optimize strand annealing and assess the potential for the microarray as a DNA-based detection system.

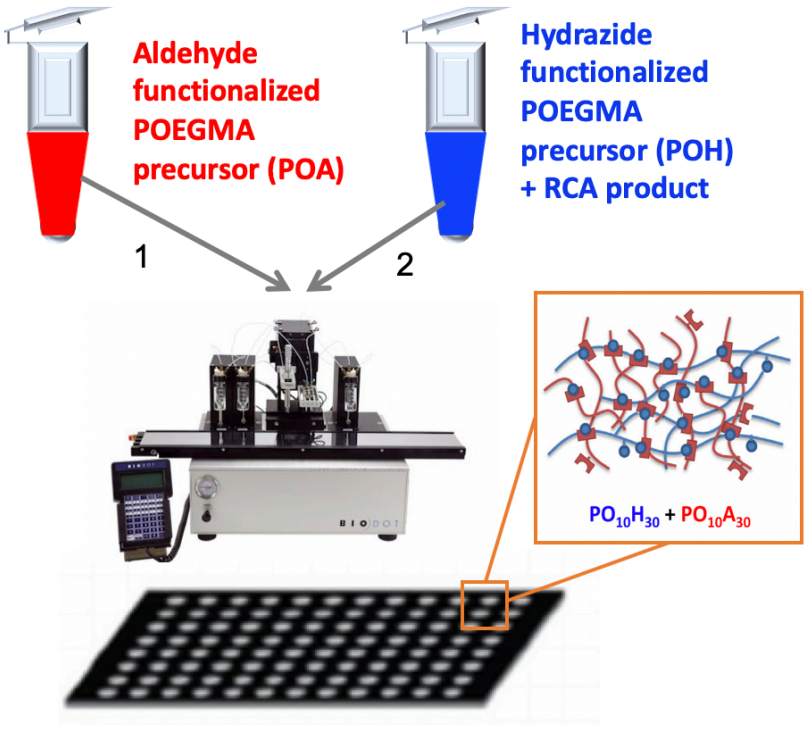

Figure 1.4. Schematic representation of the synthesis of POEGMA microarrays.

Chapter 3 describes the optimization of an inverse emulsion polymerization procedure for the encapsulation of RCA product in POEGMA microgels, schematized in Figure 1.5. Parameters such as emulsifier selection (based on HLB values), continuous phase viscosity and homogenization speed were manipulated to produce stable polymer particles that do not aggregate during polymerization. The influence of emulsifier and initiator concentration as well as temperature of the reaction on size was investigated, and a predictive model for microgel size was developed from this analysis. Finally, the encapsulation efficiency of RCA product within the microgel systems was quantified for different sized microgels.

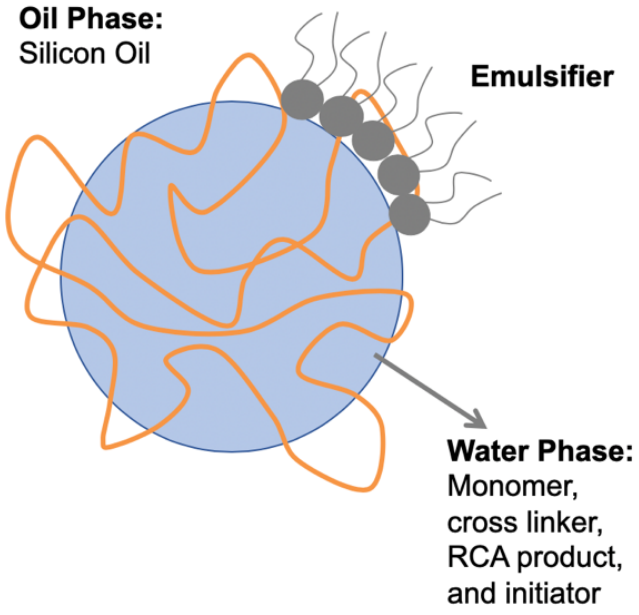

Figure 1.5. Inverse emulsion polymerization of POEGMA microgels.

Overall, this thesis aims to demonstrate the ability of POEGMA hydrogels to stabilize RCA product in two distinct structures, a step towards novel platforms that can be used as a paradigm for specific biosensing applications.

Chapter 2: Development of a printable DNA microarray stabilized within a poly(oligoethylene glycol methacrylate) hydrogel

2.1 Introduction

DNA microarrays have emerged as powerful tools in molecular biology, utilized for the simultaneous measurement of expression levels of a substantial number of genes via hybridization to immobilized complimentary "reporter" oligos.[67] Nucleic acid aptamers, engineered through repeated rounds of *in vitro* selection to bind to various molecular targets with high specificity[9, 10, 68], have been employed in DNA microarrays since their discovery expanded the recognition capability of nucleotide sequences.[68] The literature reports several aptamers for a variety of targets such as heavy metals (e.g. mercury),[69] antibiotics,[70] pathogens[71], and even select cancer cells[72]. Any of these aptamers can be directly incorporated on a substrate or conjugated to a single stranded DNA "backbone" on the substrate, thus functionalizing said material to identify a particular chemical stimulus. The applications of such microarray technologies are therefore as diverse as the aptamers employed in them, from the diagnosis of disease to the identification of toxic contaminants in food and water.

Multiple studies have looked to hydrogels as a means of physical entrapment of the nucleic acids to produce stable microarray platforms for identification of specific targets.[73, 74] The advantages of utilizing hydrogels over direct chemical immobilization are threefold. First, hydrogels provide for the physical entrapment of DNA on the substrate, eliminating the need for complex covalent linking reactions with lower than 100% incorporation efficiency.[75] Second, the hydrogel provides a hydrated environment to facilitate the diffusion and hybridization of small targets while sterically protecting the reporter from bulk environmental stresses or nuclease enzymes.[76] Finally, the 3-dimensional nature of the hydrogel expands the volume for sensing

molecules along the z-axis, improving the surface density of reporter oligos by 100 times that of traditional 2-dimensional arrays.[37]

However, a major limiting factor in using hydrogels for DNA entrapment is the long diffusion time through hydrogels for an assortment of potential chemical targets.[75] Gel modifications to increase diffusion and penetration such as the addition of hydrophilic groups[77] and the use of charged polysaccharides[78] have had some success, but typically decrease the gel stability and thus reduce or eliminate many of the benefits of the hybrid system.[79] One workaround for this unsolved problem is to focus instead on the DNA molecule being entrapped rather than the properties of the gel itself. Rolling circle amplification (RCA) product is composed of repeats of a DNA sequence linked in series to create a single stranded DNA molecule that can grow to lengths extending over several microns.[64] The use of RCA product as the DNA backbone in this system is a novel concept, and due to its large size it is expected to be physically immobilized within the hydrogel network without having to compromise diffusion associated with smaller pore sizes. Additionally, the concatemeric nature of the RCA product is expected to improve the probability of a hybridization event, ideally lowering the limit of detection and overcoming the need for signal amplification in the array.

The aim of this work is to physically entrap RCA product in a cross-linked poly(oligoethylene glycol methacrylate) (POEGMA) based hydrogel. A printable hydrogel platform will be employed wherein aldehyde functionalized POEGMA precursors and hydrazide functionalized POEGMA precursors containing RCA product are printed sequentially, allowing for hydrazone crosslinks to form around the DNA. The gel's ability to immobilize and protect the DNA sequence, as well as the potential for hybridization of short sequences to the entrapped DNA will be investigated.

2.2 Materials and Methods

2.2.1 Materials

Circular template (CT), ligation template (LT) and fluorescein-labeled probe (FP) were received from Integrated DNA Technologies (IDT) (sequences reported in Table 2.1). The DNA oligonucleotides were purified using 10% denatured polyacrylamide gel electrophoresis (dPAGE) before resuspension in PBS and storage at -80°C. T4 polynucleotide kinase (PNK), 10x PNK buffer, ATP solution, T4 DNA ligase, 10x ligase buffer, polyethylene glycol 4000 (PEG4000), dNTP mix, phi29 DNA polymerase, and 10x phi29 buffer were purchased from ThermoFisher Scientific. ULS® labeling reagent stock and ULS® labeling buffer were produced from a Ulysis® Alexa Fluor® 647 nucleic acid labeling kit obtained from ThermoFisher Scientific. Oligo(ethylene glycol) methyl ether methacrylate, M_n = 475 g/mol ($OEGMA_{475}$, 95%) and di(ethylene glycol) methyl ether methacrylate ($M(EO)_2MA$, 95%) were purchased from Sigma Aldrich and purified from added inhibitors hydroquinone monomethyl ether and butylated hydroxytoluene in a column of aluminum oxide (Sigma Aldrich, type CG-20). Acrylic acid (AA, 99%) thioglycolic acid (TGA, 98%), N,N-dimethylaminoethyl methacrylate (DMAEMA, 98%), 1,4-dioxane (99.8%) glycerol (≥99%), bovine serum albumin (BSA, >96%), Tween® 20 (protein grade) and sodium dodecyl sulfate (SDS, >98.5%) were purchased from Sigma Aldrich and used as received. 2,2-azobisisobutryic acid dimethyl ester (AIBMe, 98.5%) was purchased from Wako chemicals, adipic acid dihydrazide (ADH, 98%) was purchased from Alfa Aesar, and N'-ethyl-N-(3-dimethylaminopropyl)-carbodiimide (EDC, commercial grade) was obtained from Carbosynth, Compton CA. N-(2,2-dimethoxyethyl)methacrylamide (DMEMAm) was produced in accordance with a previously reported protocol.[45] Hi-Flow plus nitrocellulose membranes (HF12002XSS) were purchased from EMD Millipore. Saline-sodium citrate (SSC), phosphate buffered saline

(PBS), and hydrochloric acid (HCl) were purchased from Bioshop Canada Inc. at 20x, 10x, and 6.0N liquid concentrate (respectively) and diluted in Milli-Q grade distilled deionized water (DIW) as needed.

Table 2.1. Sequences of Oligonucleotides Utilized to Generate RCA Product and Detect DNA Hybridization

Oligonucleotide Abbreviation	Sequence (5' – 3')
CT	GAT CGT AGA CAA GAT GAT ACA GCA TTG AAG TCG AGG GTG TAT GAT GTG GTA AAG TAA GTG
LT	TT GTC TAC GAT CCA CTT ACT TT AC
FP	FAM/-AAA GTA AGT GGA TCG TAG AC

2.2.2 Preparation of the circular DNA template

Circular DNA was synthesized via ligation of the ends of a linear, single stranded DNA sequence (CT, Table 2.1). To begin, the template was first phosphorylated at the 5' end by action of T4 PNK. 1000 pmol of linear precursor was mixed with 15 U of PNK and 1.5 mM of ATP in 1x PNK buffer (diluted from 10x in nuclease free water) to form a 100µL reaction mixture. The mixture was incubated at 37°C for 35 minutes and subsequently heated to 90°C for 5 minutes to denature the enzyme and terminate the reaction. Following phosphorylation, ligation was executed with T4 DNA ligase and a single stranded DNA sequence complimentary to CT at the site of ligation (LT, Table 2.1). The 100µL PNK reaction mixture was first combined with 1100 pmol of LT, heated at 90°C for 1 minute and then cooled to room temperature for 20 minutes to promote strand annealing. Following cooling, 5 U of T4 DNA ligase and 30 µL of PEG4000 were added to the reaction. The final volume was brought up to 300µL by addition of 30 µL of 10x T4 DNA ligase buffer and 124 µL of nuclease free water. The reaction was incubated at room temperature for 2 hours, after which the DNA was isolated by conventional ethanol precipitation. Circular DNA

was separated from linear CT and LT by 10% dPAGE and quantified by measuring absorbance at 260 nm using the Tecan Infinite® M200 plate reader.

2.2.3 Synthesis of RCA product

Generation of RCA product was carried out by extending LT with free dNTP's using phi29 DNA polymerase in a 100µL reaction volume. Briefly, 28 pmol of circularized CT was mixed with 25 pmol of LT, 0.125 µmol of dNTP's and 25 U of phi29 DNA polymerase in 2.5x phi29 buffer (diluted from 10x in DIW). The reaction was incubated at 37°C for 1 hour, and successively heated at 90°C for 5 minutes to denature the enzyme. RCA product was purified from the reaction mixture in a 100 kDa Amicon® Ultra-0.5 mL centrifugal filter and resuspended in 100µL of 10 mM PBS. As CT was added in excess, it was assumed that the quantity of RCA product formed was equal to the amount of LT added (each product molecule extending from a single LT primer molecule), making the final concentration of RCA product 0.25 pmol/µL.

2.2.4 Synthesis and functionalization of POEGMA polymers

Hydrazide-functionalized POEGMA polymer (POH) was prepared as follows. $M(EO)_2MA$ (3.1 g, 16.5 mmol), $OEGMA_{475}$ (0.9 g, 1.9 mmol), AIBMe (37 mg, 0.16 mmol), TGA (7.5 µL, 0.15 mmol) and AA (0.55 g, 7.6 mmol) were added to 20 mL of 1,4-dioxane in a 50 mL Schlenk flask. The system was purged with nitrogen for 30 minutes and subsequently sealed and allowed to react for 4 hours in a 75°C oil bath under magnetic stirring. After the reaction, solvent was removed by rotary evaporation and the residual poly(ethylene glycol methacrylate-co-acrylic acid) polymer was dissolved in 100 mL of DIW water. The carboxylic acid groups were converted to hydrazide groups by adding 4.33 g (24.8 mmol) of ADH and adjusting the pH to 4.75 with 0.1 M HCl. To initiate the reaction, 1.93 g (12.4 mmol) of EDC was added to the flask and the solution

was maintained at pH 4.75 over 4 hours by dropwise addition of 0.1 M HCl. The mixture was left stirring at room temperature overnight before being purified via 6 cycles of dialysis (6 hours/cycle) against DIW and lyophilized to dryness. The polymer was weighed and diluted to 20 wt% in 10 mM PBS and stored at 4°C.

Cationic hydrazide-functionalized POEGMA (POH^+) was prepared in a similar fashion, although DMEAMA (1.3 g, 7.5 mmol) was also introduced to the comonomer mixture and the AA content was increased to 0.75 g (10.4 mmol) to maintain an equivalent number of AA functional groups per chain. All other quantities and procedural steps remained the same.

Neutral and anionic aldehyde-functionalized POEGMA (POA and POA^-, respectively) were synthesized following the same procedure as that of POH, but with acetal functional monomers added to the initial reaction mixture. For neutral POA, $M(EO)_2MA$ (3.1 g, 16.5 mmol), $OEGMA_{475}$ (0.9 g, 1.9 mmol), AIBMe (37 mg, 0.16 mmol), TGA (7.5 µL, 0.15 mmol), and DMAEAm (1.3 g, 7.5 mmol) were added to 20 mL of 1,4-dioxane in a 50 mL Schlenk flask. For anionic POA, the procedure was modified slightly to include AA(0.52g, 7.5 mmol) and more DMAEAm content (1.8 g) to ensure an equivalent mol% of aldehyde groups per chain. Following evaporation of the solvent, acetal groups were converted to aldehyde groups via acid hydrolysis. Residual poly(oligo ethylene glycol methacrylate-co-*N*-2,2-dimethoxyethyl methacrylamide) was dissolved in 100 mL of 1.0 M HCl. The resultant solution was left stirring at room temperature overnight before being dialyzed against DIW for 6 cycles (6 hours/cycle) and lyophilized to dryness.

2.2.5 Printing POEGMA-RCA product microarrays

Aldehyde and hydrazide functionalized POEGMA precursors were printed sequentially onto microzones of a nitrocellulose membrane to form a thin, crosslinked hydrogel array. To form

the printer "ink", each of the polymers (POA, POA^-, POH, and POH^+) were diluted to 6wt% in 10 mM PBS containing 5wt% glycerol and subsequently filtered through a 0.45 µm syringe filter. POH and POH^+ polymers were made both without and with purified RCA product at a concentration of 0.025 pmol/µL. To make the substrate, a 96 well pattern with 3 mm diameter wells and a 9 mm inter-well distance was printed onto an EMD Millipore nitrocellulose membrane with a Xerox ColorQube 8570 N wax printer. The hydrophobic wax barrier was melted into the substrate by heating the membrane for 3 minutes in a 120°C oven. The polymer inks were loaded into separate lines of a Biojet HR™ printer, and 2 µL of POA immediately followed by 2 µL of POH (with or without RCA product) were dispensed onto each well. The films were left to dry at room temperature before further analysis.

2.2.6 Visualization of printed RCA product

RCA product was labeled with fluorescent Alexa Fluor® 647 dye and imaged on the ChemiDoc™ to assess printing consistency. Firstly, purified RCA product was precipitated via standard ethanol precipitation and resuspended in 10 µL of Alexa Fluor® 647 ULS® labeling reagent stock and 50 µL of ULS® labeling buffer. The mixture was incubated at 80°C for 15 minutes before halting the reaction by holding it in an ice bath for 5 minutes. Labeled RCA product was isolated from any excess labeling reagent by centrifugation in a 100 kDa Amicon® Ultra-0.5 mL spin column and resuspended in 100 µL of 10 mM PBS. RCA product was added to POH and printed onto nitrocellulose substrate as described in section 2.2.5 (0.05 pmol RCA product/microzone). Following 2 hours of drying, the substrate was imaged using the Alexa 647 channel on the ChemiDoc™. The pixel intensity of each microzone was determined via image analysis on ImageJ software.

2.2.7 Printed RCA product immobilization assay

Purified Alexa-labeled RCA product was diluted in 10 mM PBS to 0.025 pmol/µL. Three separate nitrocellulose substrates were prepared by either printing 2 µL/microzone of RCA product in PBS, 2 µL/microzone of RCA product in POH, or 2 µL/microzone of POA followed by 2µL/microzone of RCA product in POH. The three substrates were left to dry at room temperature for 2 hours, and then washed in 5xSSC + 0.1 wt% Tween20 for 3 cycles of 20-minute washes on a shaker plate at 350 rpm, with buffer being replaced after each cycle. After each cycle, the wet substrate was imaged using the Alexa 647 channel on the ChemiDoc™ and an average pixel intensity across all microzones was calculated from analysis on ImageJ software.

2.2.8 Printed RCA product hybridization assay

POEGMA-RCA product microarrays were printed as described in section 2.2.5. Fluorescein tagged probes complimentary to the RCA product (FP, Table 2.1) were diluted as summarized in Table 2.2 in either i) 10 mM PBS or ii) hybridization buffer composed of 5x SSC, 1wt% BSA and 0.02wt% SDS. The microarray was either pre-soaked in hybridization buffer for 30 min and dried before use or used in its original form. 5 µL of probe was added to each microzone and the system was allowed to hybridize for either 30 min or 2 hours at room temperature or at 44°C. Following hybridization, washes were performed in wash buffer (2x SSC with 0.1wt% SDS) on a shaker plate at 350 rpm for 30 minutes at room temperature. Several different combinations of the above conditions were investigated to identify an optimal hybridization platform.

In some instances, different agitation strategies were tested following washing to improve extraction of unhybridized probe. The membrane was placed in wash buffer within a falcon tube and centrifuged at 1000G or placed in an ultrasonic bath for varying amounts of time before

imaging. Additionally, hybridized membrane was suspended in a 10% dPAGE gel and subjected to a 1000-volt electric field for 1 hour to electrostatically remove excess probe.

Following hybridization and washing, the substrates were imaged using the fluorescein channel on the ChemiDoc™ and the ratio of pixel intensity of the POEGMA-RCA product ("signal") in comparison to the intensity of POEGMA without RCA product ("noise") was determined using ImageJ software.

Table 2.2. Fluorescein-labeled Probe Concentrations Utilized in Hybridization Assays

Column of 96-well microarray	Concentration (pmol/µL)
1	0.02
2	0.1
3	0.2
4	0.4
5	1.2
6	1.6
7	2
8	2.4
9	3.2
10	3.6
11	5
12	6

2.3 Results and Discussion

2.3.1 Printing a consistent DNA Microarray

Visual inspection and ImageJ analysis of the dried POEGMA hydrogel containing Alexa-labeled RCA product demonstrates that the Biojet HR™ printer consistently distributes RCA product across all microzones. Figure 2.1 depicts the average fluorescence intensity (after subtraction of background) across three microzones for 12 columns of the 96 well pattern, with the un-modified image in the inset. With an average intensity of 243 and a standard deviation of 13, the coefficient of variation in this dataset is merely 5.5%, indicating uniform printing among

all microzones. Consistency is vital for an accurate array; if certain wells contained a disproportionately high amount of RCA product, hybridization events could be logically heightened to produce a signal indicative of more target than is truly present. The opposite is possible for wells containing an abnormally low mass of RCA product. This result supports the goal for use of this platform as a microarray in biosensing applications, as low variability amongst microzones allows for direct comparison of zones within a single assay and comparison to established standards.

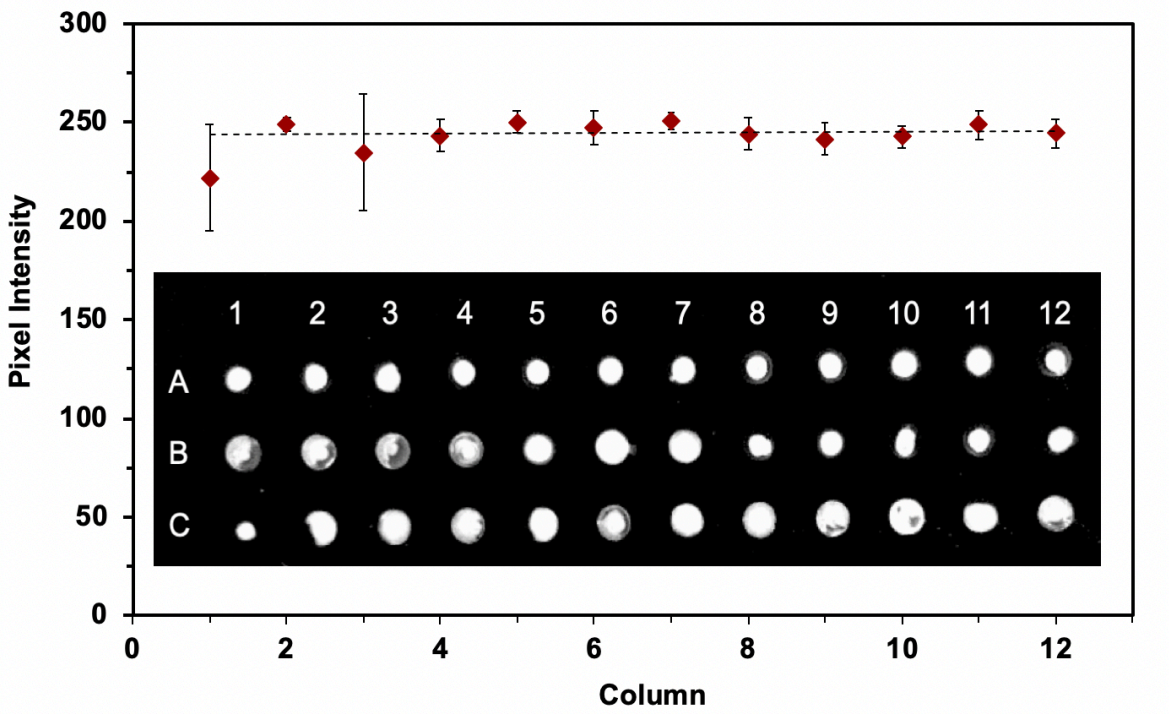

Figure 2.1 Average pixel intensity of Alexa-labeled RCA product printed in a POEGMA hydrogel on a 96-well nitrocellulose membrane. Microzones A through C in each column are replicate samples. Data are column means ± 1 s.d (n = 3). Inset: Image of the substrate taken on a ChemiDoc™ gel imaging system.

It is important to note that the accuracy of microzone comparisons would be further improved with a lower coefficient of variation amongst all zones, which is possible with an enhanced printing technique. In this investigation, the printer ran through all 36 wells without

nozzle cleaning or purging. Any minor nozzle obstructions that arose during the experiment could have led to regions of lower than average volume deposition and fluorescence (e.g. well C.1, Figure 2.1) followed by regions of above average volume as pressure buildup clears the nozzle. Due to this influence, it would be worth investigating the printing consistency after introducing an additional 2-3 second purge step between each microzone, or after every few microzones, to see if an improvement is noticed.

2.3.2 Immobilizing RCA product in a crosslinked POEGMA hydrogel

Analysis of the preserved fluorescence intensity after several wash cycles of Alexa-labeled RCA product printed in PBS, in POH alone, and in a crosslinked POEGMA hydrogel reveal the importance of the hydrogel for stabilization of RCA product on the substrate. As Figure 2.2 demonstrates, RCA product within the POEGMA hydrogel retained 95% of the initial fluorescence after the 3rd cycle of washing in 5xSSC + 0.1 wt% Tween20. Conversely, RCA product printed on its own or within POH (polymer unable to crosslink) retained less than 30% of the initial fluorescence after the 3rd wash cycle. These results dictate the value of the hydrazone crosslinking chemistry for immobilization of RCA product and demonstrate the stability of this platform against environmental disturbances.

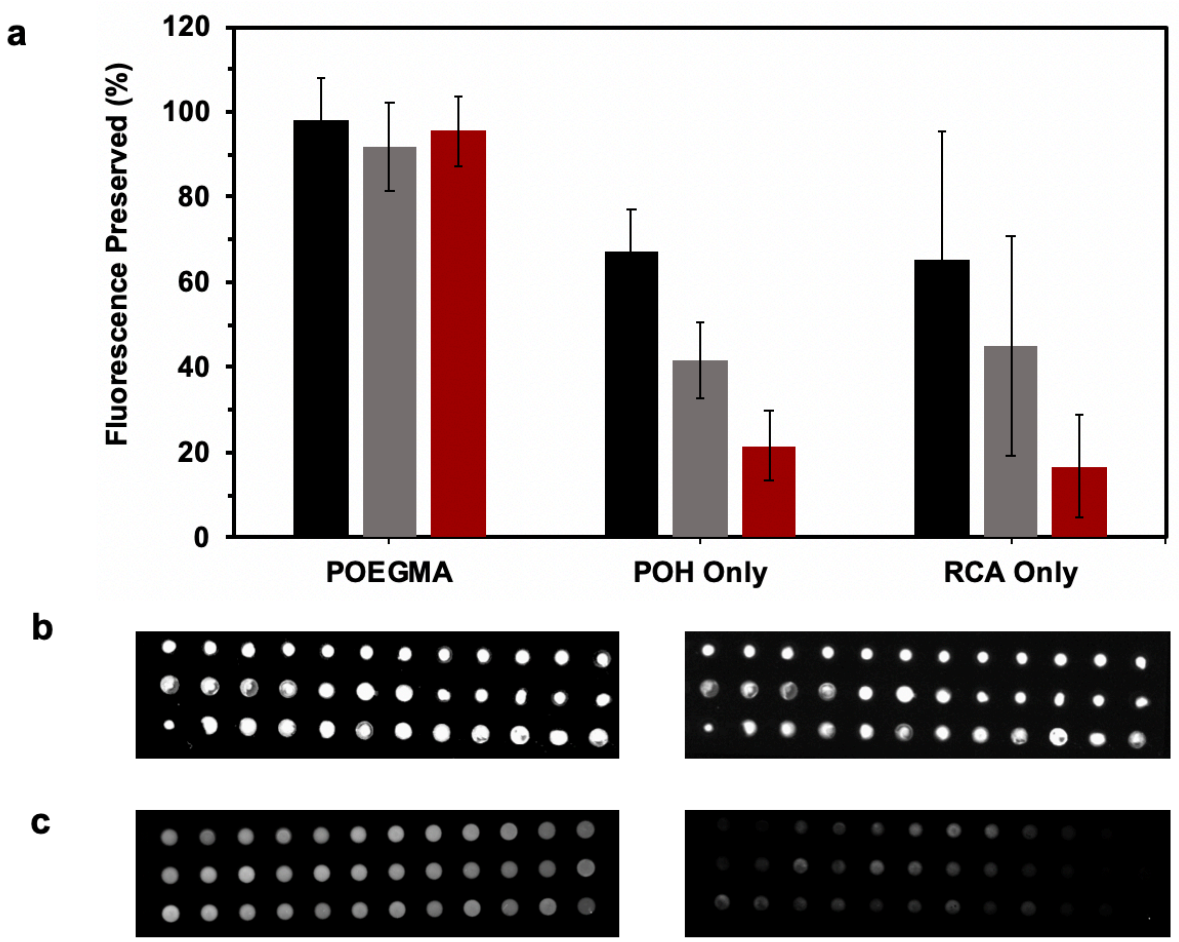

Figure 2.2 (a) Percentage of preserved fluorescence after 1 wash cycle (■) 2 wash cycles (■) and 3 wash cycles (■) for Alexa-labeled RCA product printed and dried in a POEGMA hydrogel, POH polymer, and without polymer support. Data are means ± 1 s.d (n = 3). **(b)** Alexa labeled RCA product in a POEGMA hydrogel before washing (left) and after the third wash cycle (right). **(c)** Alexa labeled RCA product on nitrocellulose before washing (left) and after the third wash cycle (right).

2.3.3 Optimizing a hybridization assay for the printed RCA product

Initial attempts at hybridizing the fluorescein-labeled probe to printed RCA product were unsuccessful, with no discernable difference between the printed RCA product and the negative control yielding a signal-to-noise ratio of ~1 across all microzones. Probes were suspended in 10 mM PBS at concentrations summarized in Table 2.2, pipetted onto each microzone and left to

hybridize for 30 minutes at room temperature before being washed in wash buffer for 30 minutes. The result is displayed in Figure 2.3 below. With a high background signal, it is impossible to discern whether hybridization is occurring, or if the signal from wells with RCA product is merely the result of non-specific probe interactions.

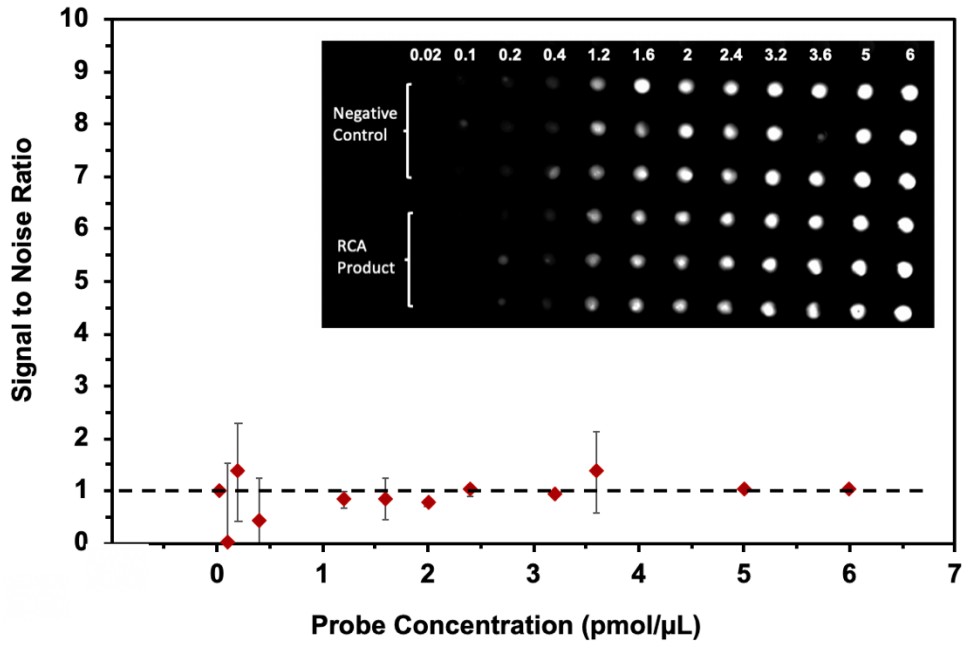

Figure 2.3 Ratio of the pixel intensity for FP incubated in a POEGMA hydrogel containing RCA product (signal) to a POEGMA hydrogel without DNA (noise). Data are means ± 1 s.d (n = 3). Inset: Image of the substrate taken on a ChemiDoc™ gel imaging system.

To distinguish between hybridization events and non-specific probe attachment, several experiments were systematically executed in an attempt to reduce the background signal and achieve a greater signal/noise ratio. From this initial result, it was hypothesized that unhybridized FP could be preserved on the substrate following washing for one of three reasons: (1) interactions with the nitrocellulose substrate; (2) physical entrapment within the densely crosslinked gel; or (3) electrostatic/affinity interactions with the polymers. The remainder of this section highlights strategies explored to investigate these effects and address them via polymer design.

Influence of the nitrocellulose substrate on FP Retention

Prior to making significant adjustments to the system and hybridization protocol, native nitrocellulose was assessed to determine if the underlying substrate had a significant role in non-specific adsorption. To start, 5 µL of FP was deposited onto microzones with no printed film (bare nitrocellulose) and microzones containing dried POEGMA hydrogels. The system was left for 30 minutes to mimic a typical hybridization experiment before being washed in wash buffer for 30 minutes. Figure 2.4 demonstrates the average fluorescence intensity over different probe concentrations for both systems. It is evident that at higher FP concentrations, the substrate with a dried hydrogel retains an appreciably greater amount of probe than the native nitrocellulose substrate. In fact, with almost negligible fluorescence detected in the microzones in which POEGMA is absent, it can be concluded that washing of the substrate was effective at removing unhybridized probe from the nitrocellulose paper. This result confirms that nitrocellulose was a suitable choice for the substrate in this system, as it does not impart any influence on the probe that would amplify the background signals.

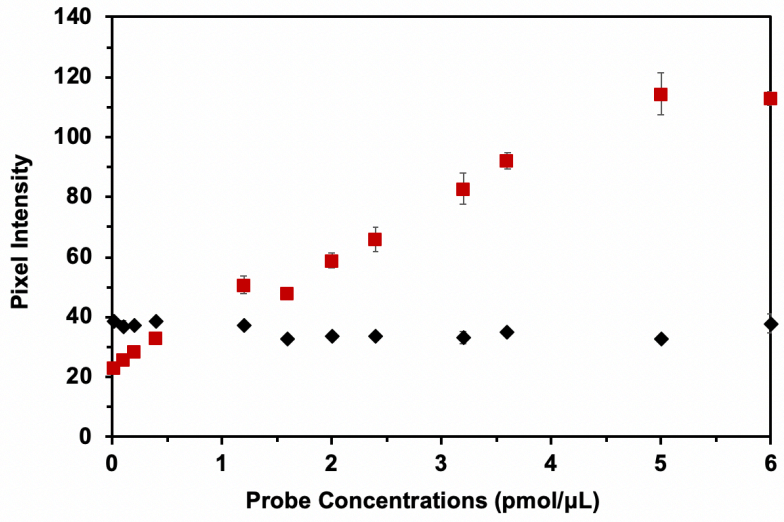

Figure 2.4 Pixel intensity of nitrocellulose membrane (◆) and nitrocellulose with a printed POEGMA hydrogel (■) following incubation with FP for 30 minutes. Data are means ± 1 s.d.

Influence of Hydrogel Thickness on FP Retention

With nitrocellulose eliminated as the cause for non-specific FP binding, subsequent experiments involved adjustments to the hydrogel itself. Thinner and less crosslinked POEGMA gels were explored with the notion that shrinking the diffusion pathways in the z-direction and "opening up" the pores would limit physical entanglement of the probe and facilitate probe removal during washing. In the first trial, POA was printed onto the substrate and allowed to dry completely before the POH/RCA layer was deposited. By allowing POA to dry, it was assumed that only the top regions of the polymer would be rehydrated and participate in crosslinking, generating a thinner, less cross-linked gel due to inefficient mixing of precursors. The substrate was imaged following hybridization and washing, and the result is depicted in Figure 2.5 (a).

Alternately, using a different approach to make a thinner gel, POA and POH layers were printed in a lower volume (1 μL per microzone) while the mass of RCA remained unchanged at 0.05 pmol per microzone by using POH "ink" at an RCA concentration of 0.05 pmol/μL. Figure 2.5(b) demonstrates this result. With a signal/noise ratio close to 1 for both attempts, it was concluded that non-specific probe attachments could not be overcome by employing a thinner hydrogel. This could be due to the nature of the interactions or simply due to the fact that physical interactions are more intense than imagined, such that opening up the gel matrix was not enough to compensate. Further decreasing the thickness or crosslinking density was not investigated, as it is likely that a lower crosslinked gel lacks the protective ability required to fully stabilize RCA product. Since no improvement in background was noted in comparison with the base case (Figure 2.3), the original gel system was revisited in future studies due to its proven ability to protect RCA product from environmental agents.

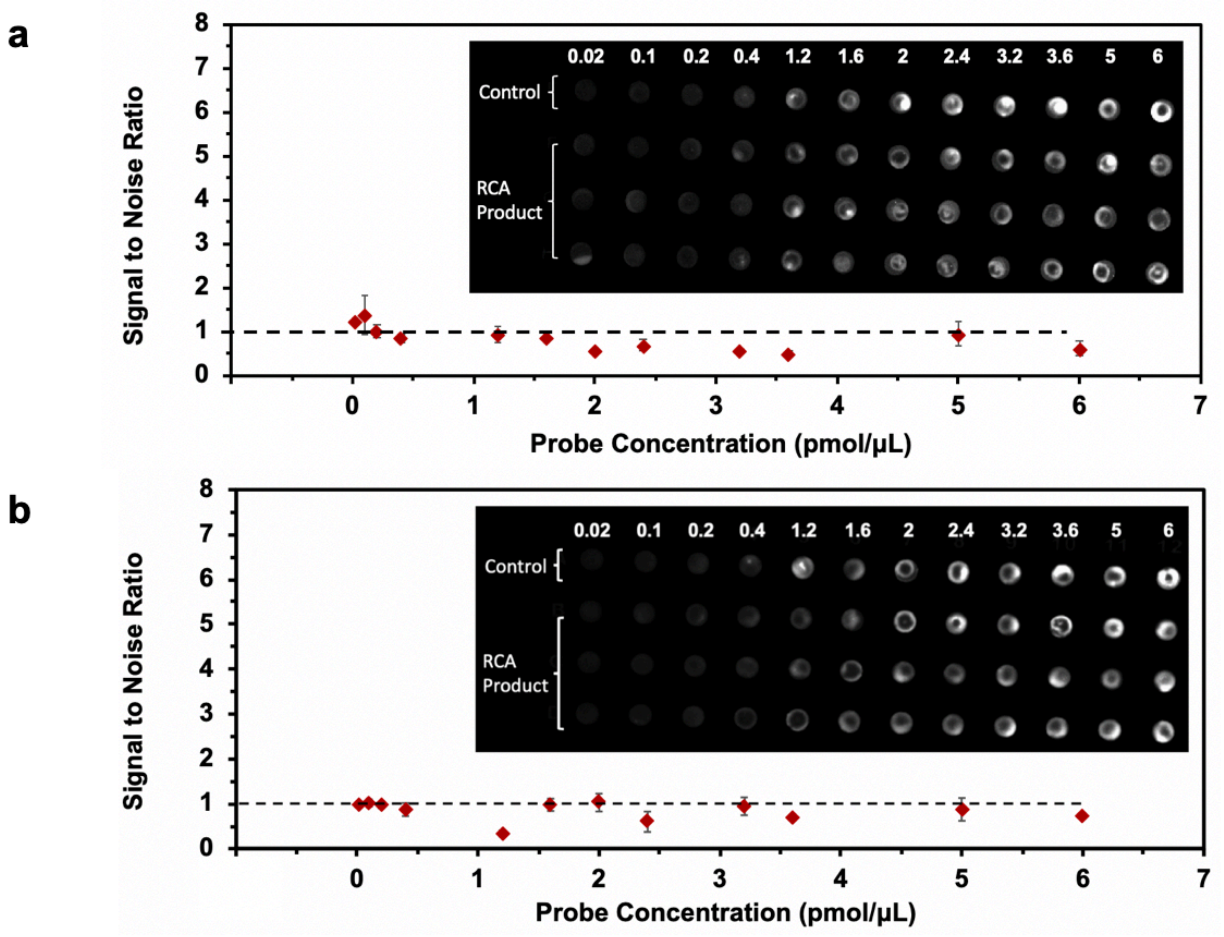

Figure 2.5 (a) Ratio of the pixel intensity for FP incubated in a lower crosslinked POEGMA hydrogel containing 0.05 pmol RCA product per microzone (signal) to a POEGMA hydrogel without DNA (noise). Inset: Image of the substrate taken on a ChemiDoc™ gel imaging system. **(b)** Ratio of the pixel intensity for FP incubated in a thin-layer POEGMA hydrogel containing 0.05 pmol RCA product per microzone (signal) to a POEGMA hydrogel without DNA (noise). Inset: Image of the substrate taken on a ChemiDoc™ gel imaging system. Data are means ± 1 s.d (n = 3).

Increasing the intensity of washing steps to improve unhybridized FP removal

With the thinner gels failing to reduce background signals or provide insight as to the reasons for the high probe retention, the next investigation sought to determine the nature of probe entrapment within the hydrogel. It was hypothesized that simple washing on a shaker plate was insufficient for removal of unbound FP, potentially due to steric barriers caused by physical

entanglement of the probe within the gel, or the presence of capillary forces or affinity interactions within the hydrogel pores that pull the probe inward. To try to overcome such obstacles, different extraction forces were employed to more vigorously remove the non-specifically bound probe from the printed hydrogel. The first trial exploited energy from ultrasonic sound waves. It was theorized that, if physical entanglements were responsible for retaining the probe, increasing the energetics of the washing step could disrupt the system enough to dislodge the entangled probe. Squares of 4 microzones were hybridized with 5 µL of 2 pmol/µL FP for 30 minutes before being submerged in wash buffer within an Eppendorf tube and sonicated. 2 pmol/µL FP was selected for the experiment, as it is well-established that a suitable target molecule concentration is extremely important for obtaining clear signals in hybridization assays.[80] Too low of a concentration can yield a low signal (microzones 1-3 in Figure 2.3), while too high of a concentration can create a high background (microzones 10-12 in Figure 2.3). To avoid both issues, an intermediate concentration from Table 2.2 was selected.

Figure 2.6 shows the average intensity of microzones with POEGMA printed alone in comparison to microzones with RCA product for different lengths of time in an ultrasonic bath. Evidently, the fluorescence intensity did not decrease with time left in the ultrasonic bath. With 100% fluorescence retained in the negative control gel after 20 minutes of sonication, it can be concluded that higher energy washing removed little to no probe from the hydrogel matrix. This result implies that steric interactions are not the main reason for non-specific FP retention, as the disturbance imparted by ultrasonic pulses was expected to overcome entanglement issues.

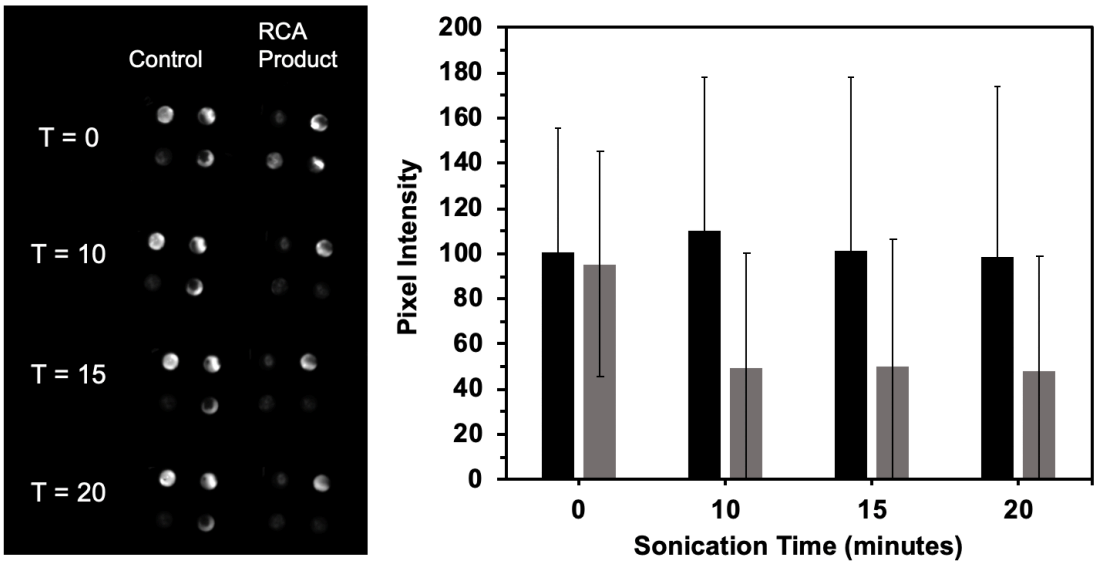

Figure 2.6. Pixel intensity of a printed POEGMA hydrogel (■) and a printed POEGMA hydrogel containing RCA product (■) following incubation with FP for 30 minutes and sonication in wash buffer for variable amounts of time. Data are means ± 1 s.d (n = 3).

A similar experiment was conducted wherein gravitational forces generated by centrifugation were employed to "pull" unhybridized FP from the hydrogel. Squares of 4 microzones were hybridized with 2 pmol/μL FP (a concentration selected for the same logic as described above) for 30 minutes before being submerged in wash buffer within an Eppendorf tube (microzones facing the outer wall of the tube) and centrifuged. Figure 2.7 shows the average fluorescence intensity of microzones with POEGMA printed alone in comparison to microzones with RCA product in POEGMA for different lengths of centrifugation. Not only is the difference between signal and noise insignificant, but more notably the average fluorescence intensity per substrate is retained even after extended periods of centrifugation. Additional attempts at greater rotational speeds showed similar results. This indicates that the centrifugal force was not sufficient to pull any of the initially deposited probe from the POEGMA hydrogel, suggesting that the forces

holding the probe within the hydrogel are stronger than the imparted centrifugal force. One explanation for this phenomenon is the capillary forces within the pores of the hydrogel. At small length scales – as is the case within the pores of a POEGMA hydrogel – capillary forces far surpass gravitational forces.[81] Thus, it is possible that the probe is being held in the hydrogel by capillary forces that must be overcome during either extraction or hybridization in order to amplify the signal to noise ratio.

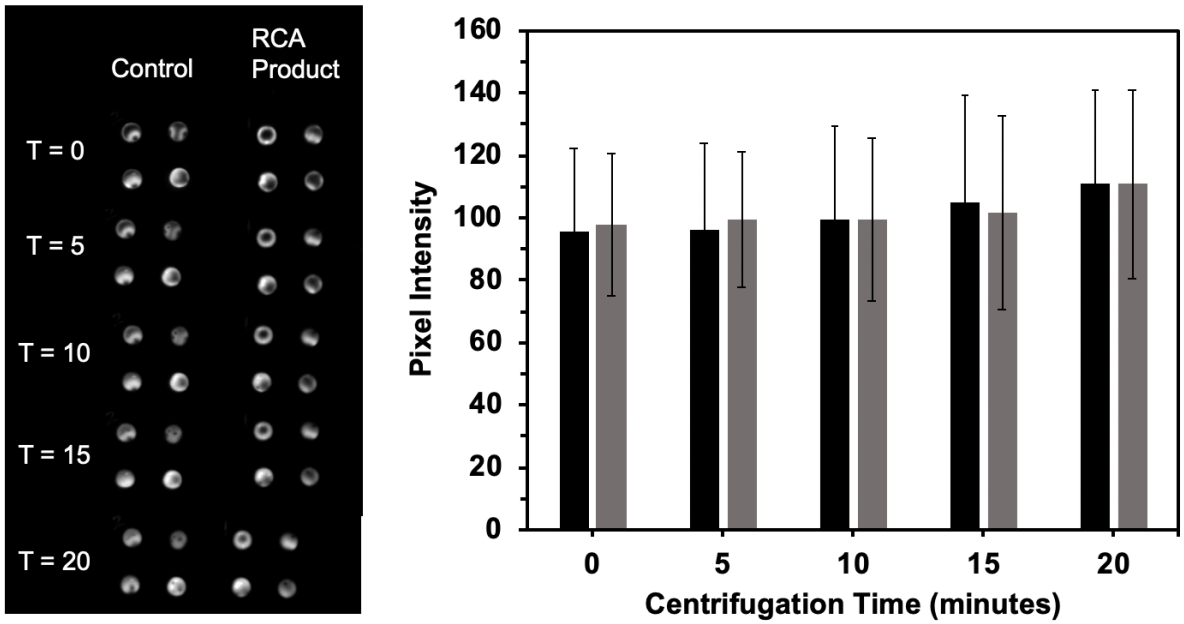

Figure 2.7. Pixel intensity of a printed POEGMA hydrogel (■) and a printed POEGMA hydrogel containing RCA product (■) following incubation with FP for 30 minutes and centrifugation in wash buffer for variable amounts of time. Data are means $\pm$ 1 s.d (n = 3).

To apply more direct and stronger forces to the hydrogel to test the above theory, the substrate was placed within a dPAGE gel following 30 minutes of hybridization in 2 pmol/µL FP and subjected to a 1000V electric field. By utilizing equations 2.1 and 2.2 below and assuming a net charge (q_{probe}) of 20(e^-) on a 20-base probe, the force acting on a single probe molecule is estimated at $1.07\,x\,10^{-14}$ N, which is over 100 times greater than the gravitational force

(~9.1 $x\ 10^{-17}$ N) acting on a single probe molecule at 1000G's. Figure 2.8 depicts the fluorescence intensity after removal from the dPAGE gel. Significantly lower fluorescence was observed in the microzones containing no RCA product, while some fluorescence retained in the wells where hybridization is expected to have occurred. Evidently, the magnitude of the electric field was enough to pull unhybridized probe from the negative control hydrogel. This is consistent with findings from Xiao et. al, in which probe absorbed into a polyacrylamide gel microarray could not be washed away by agitating in appropriate wash buffer but was successfully removed by an applied electric field.[73] Additionally, the signal-to-noise ratio (>1) is indicative of hybridization, however the non-uniform distribution of fluorescence within these zones implies that perhaps conditions were not optimized to hybridize the majority of the probe before the electric field was applied.

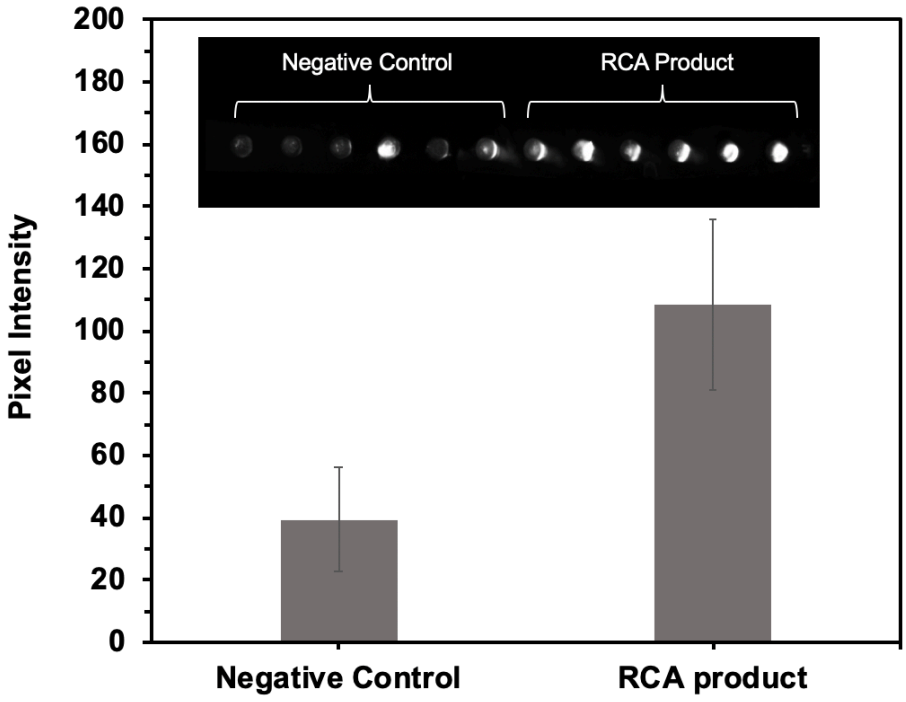

Figure 2.8. Pixel intensity of a printed POEGMA hydrogel and a printed POEGMA hydrogel containing RCA product following incubation with FP for 30 minutes and extraction in a 10% dPAGE gel at 1000 volts. Data are means $\pm$ 1 s.d (n = 6).

$$E = \frac{V}{d_{plates}} \tag{2.1}$$

$$F = Eq_{probe} \tag{2.2}$$

Improving hybridization conditions

Careful adjustments to the hybridization conditions (namely the choice of buffer and time for hybridization) were found to reduce background and enhance the signal to noise ratio, effectively promoting hybridization. The hybridization of probe to solid substrates, as used during southern blots, has been well established in the literature.[82] Common practice is to employ a high salt buffer equipped with blocking agents and detergents to reduce non-specific interactions of the probe with the substrate.[83] Additionally, several sources report "pre-hybridization", wherein the substrate is soaked in the buffer prior to hybridization to block available binding sites.[80] From these recommendations, hybridization buffer was replaced with 5x SSC, 1wt% BSA and 0.02wt% SDS which was used to dilute the probes and soak the membrane for 30 minutes before hybridizing. Following drying, the substrate was hybridized for 30 minutes and washed for 30 minutes, with Figure 2.9(a) showing the result of the assay.

While there was no improvement to the signal/noise ratio, it can be noted that there was also no increase in intensity with added probe concentration. In fact, the fluorescence detected in the microzones appears to be artifact, as regions of the substrate with extremely low concentrations of FP show similar intensities. This implies that little to no probe is being retained within the hydrogel, with prior blocking greatly reducing background. Successful blocking can likely be attributed to the BSA; at 66.5 kDa in size and a charge of -18(e) at neutral pH, BSA can both sterically block the probe from diffusing into tight pores (3.3 nm in size)[50] and electrostatically

repel the negatively charged entity. Unfortunately, the low background is accompanied by a low signal in microzones containing RCA product, indicating a lack of hybridization.

To encourage hybridization events, the time for hybridization was increased from 30 minutes to 2 hours, and the result is shown in Figure 2.9(b). Increasing the hybridization time dramatically improved the signal/noise ratio at high probe concentrations, with a low background and impressive signal in the highest 4 microzones. Several reports suggest 2-4 hours are required for DNA:DNA hybridizations.[84, 85] However, it should be noted that hybridization is only possible within an aqueous environment in which probes have the mobility necessary to locate and bind to complementary targets. By depositing just 5 µL of FP per microzone, much of the water in the buffer evaporates after approximately 40 minutes, creating a dried substrate for which any additional time was irrelevant for enhancing hybridization. To compensate for this, an additional 5 µL of hybridization buffer was added to each zone every 30 minutes to ensure a fluid environment is maintained to aid in hybridization. As can be seen from Figure 2.9(b), this combination of adjustments significantly improved the signal-to-noise ratio, with blocking remaining effective at reducing background even at the longer hybridization time.

In an attempt at further improving the signal-to-noise ratio, the temperature of hybridization was augmented from room temperature to 44°C. Figure 2.9(c) summarizes this result, demonstrating a low background yet inconsistent improvements to the signal in the microzones containing complementary RCA product. Protocols for southern blots suggest to hybridize at a temperature that is 20-25°C below the melting temperature; the temperature of complementary strand separation.[85] Given that the melting temperature was calculated to be 64°C based on the ratio of A/T pairs to G/C pairs (according to equation 2.3), 44°C was selected for hybridization. In this case, the experiment is further complicated by the thermoresponsivity of the

POEGMA hydrogel system, with previous reports indicating a volume phase transition temperature (VPTT) of ~33°C (at which point the hydrogel deswells).[50] With the gel collapsing, accessibility to regions of the RCA product buried within the gel is diminished, leaving only loops of DNA that extend beyond the hydrogel available for binding. The inconsistent signal detected in microzones with RCA product suggests that RCA product does extend significantly beyond the bulk hydrogel, albeit in an erratic and highly variable manner. Due to the inconsistencies in this finding, it was recommended that hybridization in this system be pursued at room temperature moving forward.

$$T_m = 4(G:C) + 2(A:T)°C \quad (2.3)$$

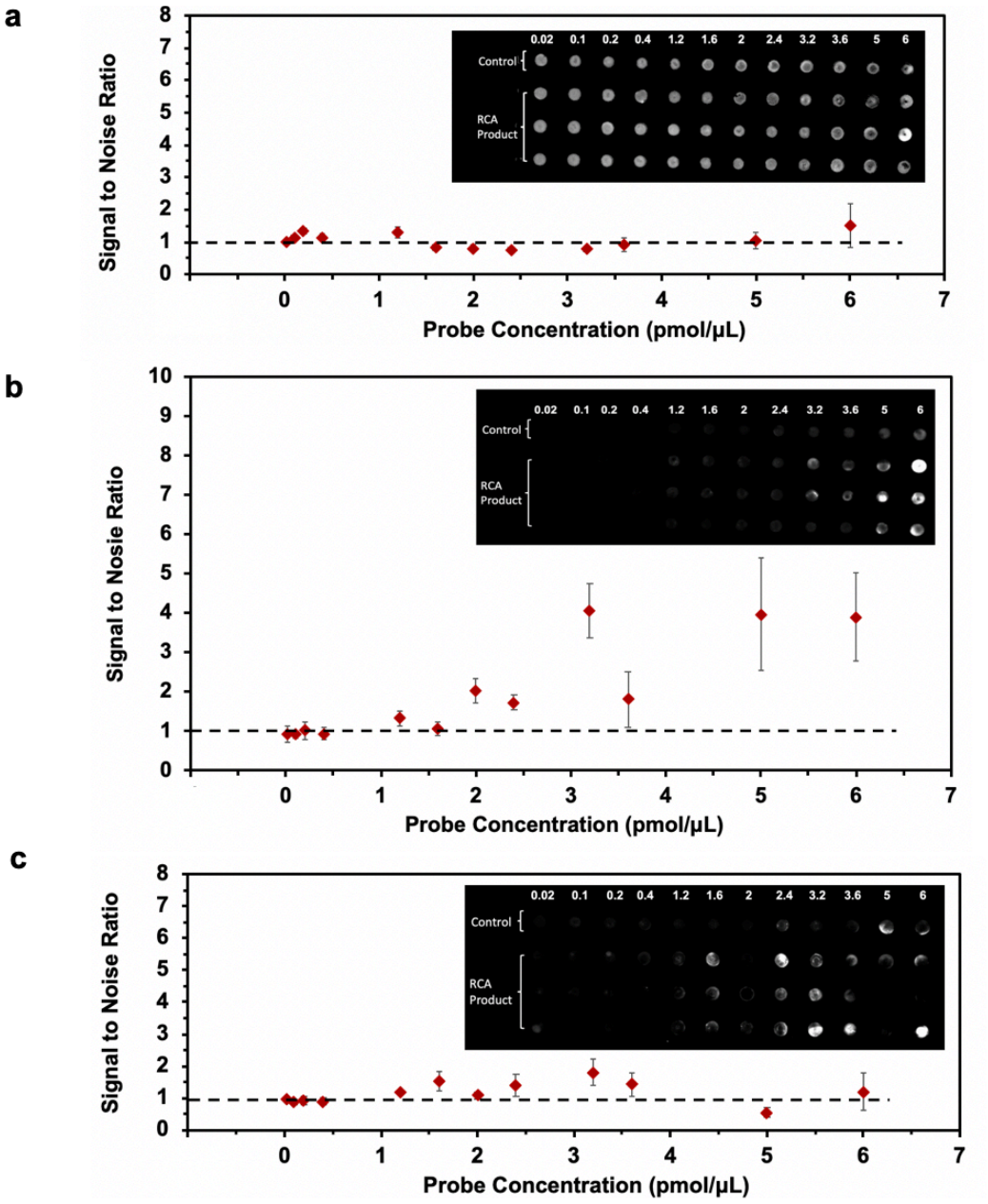

Figure 2.9 (a) Ratio of the pixel intensity for FP incubated at room temperature for 30 minutes in a BSA-blocked POEGMA hydrogel containing 0.05 pmol RCA product per microzone (signal) compared to a POEGMA hydrogel alone (noise). Inset: Image of the substrate taken on a ChemiDoc™ gel imaging system. **(b)** Ratio of the pixel intensity for FP incubated at room temperature for 2 hours in a BSA-blocked POEGMA hydrogel containing 0.05 pmol RCA product per microzone (signal) compared to a POEGMA hydrogel alone (noise). Inset: Image of the substrate taken on a ChemiDoc™ gel imaging system. **(c)** Ratio of the pixel intensity for FP incubated at 44°C for 2 hours in a BSA-blocked POEGMA hydrogel containing 0.05 pmol RCA product per microzone (signal) compared to a POEGMA hydrogel alone (noise). Inset: Image of the substrate taken on a ChemiDoc™ gel imaging system. Data are means ± 1 s.d (n = 3).

The effect of polymer charge on FP hybridization

To manipulate the orientation of RCA product within the hydrogel and investigate the influence on hybridization, polymers of different charges were investigated as precursors to the gel system. Two systems were tested: neutral POA with cationic POH, and anionic POA with neutral POH. Introducing a cationic charge was predicted to pull or spread the highly anionic RCA product, eliminating folded regions and self-interactions to increase the number of available binding sites for FP and enhance hybridization. The anionic POA was predicted to work by repelling the RCA product to upper layers of the hydrogel so more hybridization can place at the surface. The gels were printed, dried, and blocked with the improved hybridization buffer before being incubated with probe for 2 hours. The results following washing and imaging are summarized in Figure 2.10. In both cases, the signal-to-noise ratio at higher probe concentrations is comparable to that for the neutral hydrogel under the same conditions. However, the heightened ratio is noted over a larger range of probe concentrations, in comparison to the neutral hydrogel for which the ratio drops to 1 at intermediate concentrations. It is possible that the greater signal detected in the cationic system means the probe was able to "find" more complementary sites on the RCA product, indicating a better orientation with less folding in the product. In order to draw stronger conclusions from the anionic system, it would be beneficial to try hybridizing at 44°C while the gel is in a collapsed state. If the anionic polymer promotes RCA product repulsion beyond the borders of the gel, perhaps a strengthened and more consistent signal would be detected under these conditions as well.

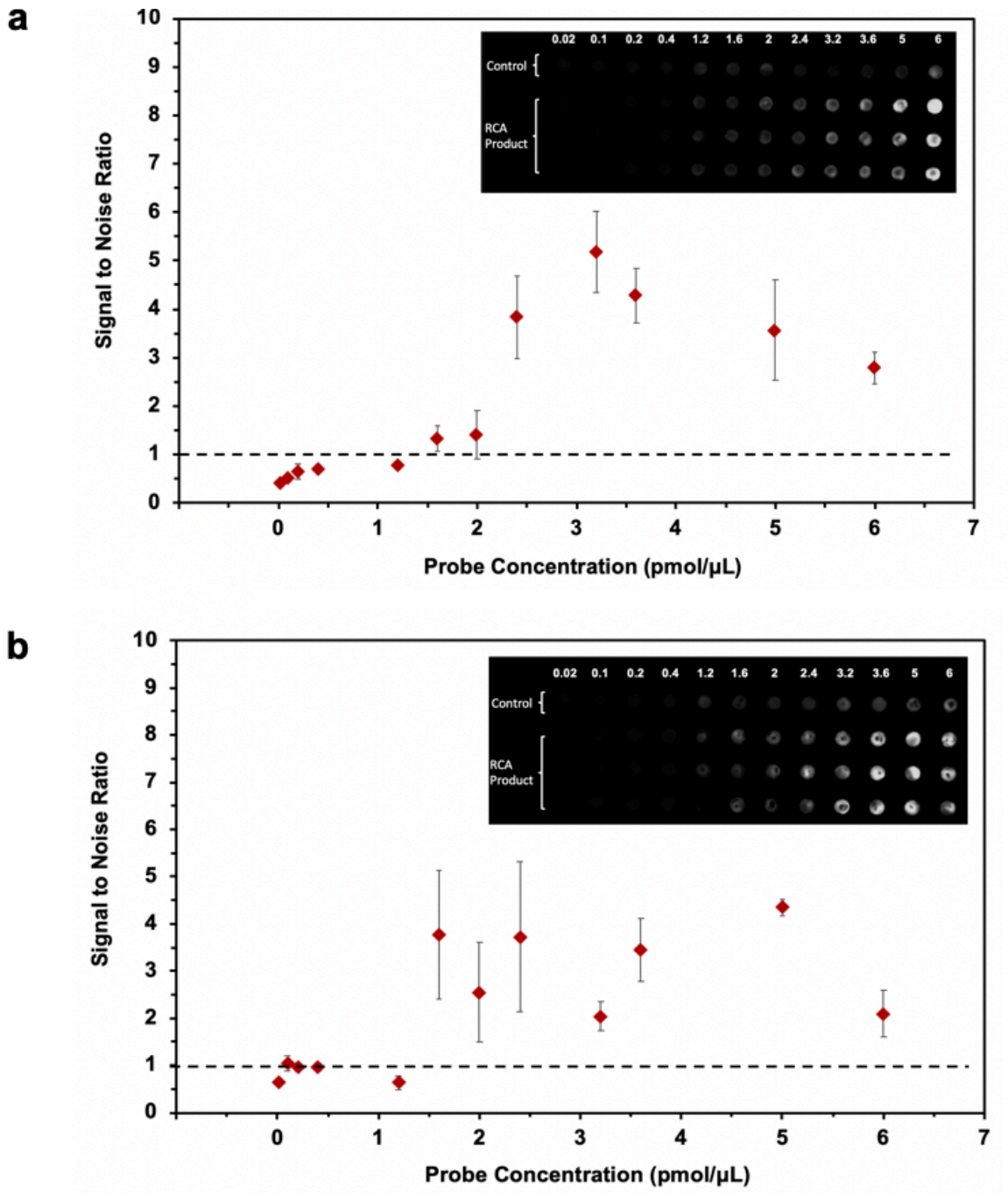

Figure 2.10 (a) Ratio of the pixel intensity for FP incubated at room temperature for 2 hours in a BSA-blocked cationic POEGMA hydrogel containing 0.05 pmol RCA product per microzone (signal) to a POEGMA hydrogel alone (noise). Inset: Image of the substrate taken on a ChemiDoc™ gel imaging system. **(b)** Ratio of the pixel intensity for FP incubated at room temperature for 2 hours in a BSA-blocked anionic POEGMA hydrogel containing 0.05 pmol RCA product per microzone (signal) to a POEGMA hydrogel alone (noise). Inset: Image of the substrate taken on a ChemiDoc™ gel imaging system. Data are means ± 1 s.d (n = 3).

2.4 Conclusions

A printable DNA microarray composed of RCA product stabilized within a POEGMA hydrogel shows promise as a stable system for target hybridization. RCA product was effectively and consistently printed onto nitrocellulose substrate with gel precursors, showing a low coefficient of variation across 36 microzones. Furthermore, the hydrogel successfully stabilized the RCA product, holding it in place even after 3 cycles of washing in a high salt buffer. Hybridization of complementary probe to printed RCA product was challenging due to the high background signal generated by strong non-specific probe interactions with the hydrogel. Such interactions were overcome by blocking the hydrogel with BSA prior to hybridization, elongating the hybridization time and maintaining aqueous conditions for the duration of the incubation. Modifications to the hybridization scheme increased the signal to noise ratio 4x at high probe concentrations (5-6 pmol/μL) and 2x at intermediate probe concentrations (2-4 pmol/μL). Although improvements were noted, further studies should be conducted to improve RCA access to the probe and thus enhance the signal generated from hybridization events. Moving forward, it would be worth exploring the effects of incorporating different charge densities on the polymer precursors (particularly anionic POA) and performing hybridization at temperatures above the VPTT and close to the melting temperature. We hypothesize that an optimum can be reached wherein the RCA product is repelled toward the surface and non-specific absorption is supressed due to hydrogel shrinkage, yielding a strong signal-to-noise ratio across all probe concentrations that would support the use of this platform in biosensing applications.

Chapter 3: Synthesis and characterization of poly(oligoethylene glycol methacrylate) microgels containing Rolling Circle Amplification product for concentration of target molecules

3.1 Introduction

Continuous-flow collection devices are of value for the concentration and detection of ultralow concentration target analytes in solution, thus enabling the earlier detection of diseases and simplifying the processing steps in analysis of complex samples. In a typical continuous flow system, the sample of interest is passed through an affinity column that collects the desired target; following, it can be eluted using a low volume of buffer at concentrations that render it far easier to detect. Affinity columns can be general in nature, like silica-based columns that favourably adsorb DNA with any sequence[86], or highly specific, allowing for collection of particular DNA sequences or chemical targets.

With the discovery of aptamers – specifically evolved DNA sequences that preferentially self-anneal to form desired structures[9, 10]– the recognition power of nucleic acids has grown significantly. Not only can DNA be utilized to catch complementary sequences, but also particular markers like β-secretase[87] (Alzheimer's disease), epidermal growth factor receptor[88] (breast and lung cancer), heavy metals[69], pathogens[89], and more. The sheer volume of recognition events reported makes nucleic acid-based affinity columns particularly attractive. Affinity chromatography with DNA employed for target capture is not a new concept; nearly 50 years ago, Schaller et al. reported agarose gels with immobilized phage DNA for capture of DNA binding enzymes.[90] In 1999, aptamers were first reported as the affinity ligand in chromatographic separation with the purification of human L-selectin.[91] In recent years, a commonly reported theme in nucleic acid concentration devices involves covalent fixation of aptamers to microparticle

supports that can be packed into a column for extraction and concentration of distinct targets.[92-94] Unfortunately, there are issues with stability/longevity of such columns, and the complex chemistry of fabrication conferred by covalent linkage of aptamers to the support is expensive and time-consuming.

Micron sized hydrogels (microgels) are an appealing material for the support of nucleic acids in affinity columns. Due to their highly porous structures, hydrogels can allow for diffusion of targets *into* the microparticle, simultaneously sterically protecting the delicate sensing element from nuclease degradation and enhancing the binding capacity by expanding the surface area for DNA immobilization to the interior of the particle. The dual benefits of employing a microgel as opposed to solid microparticles have been heavily investigated and reported in recent years.[42, 95]

One significant drawback for conventional microgel/DNA affinity columns is the complexity of DNA incorporation into the gel. Covalent attachment is the most widely utilized method for immobilization, but requires generally complex chemistry and specific functionalized DNA in addition to reducing the ease of fabrication and scale-up.[36] Physically entrapping nucleic acids in the microgel would be preferred; however, to achieve robust immobilization, the pore size of the gel must be smaller than the length of the DNA. Conversely, shrinking the pore size to rival that of entrapped sequences or aptamers introduces diffusion difficulties for target molecules. To overcome this issue without significantly altering the microgel structure, Rolling Circle Amplification (RCA) product – a single stranded DNA molecule composed of the same sequence repeated thousands of times in tandem[64]– can be employed as the sensing element for different targets. RCA product can grow to lengths extending over several microns, making it larger than microgel pore sizes and enabling strong physical entrapment within polymer networks.[66] Furthermore, RCA product can be synthesized for any sequence of DNA, offering the flexibility

to recognize specific sequences or hybridize to complementary aptamers for the identification of more unique targets. Thus, entrapment of RCA product within microgels creates a simple and diverse platform for the affinity capture and concentration of analytes.

Herein, we present the development of poly(oligoethylene glycol methacrylate) (POEGMA) microgels containing physically entrapped RCA product. Optimization of the polymerization strategy along with the characterization of the microgel sizes and the size response to various emulsion parameters are discussed. Finally, the encapsulation efficiency of RCA product within the POEGMA microgels is analyzed.

3.2 Materials and Methods

3.2.1 Materials

Circular template (CT) and ligation template (LT) were received from Integrated DNA Technologies (IDT) (sequences reported in Table 3.1). The DNA oligonucleotides were purified using 10% denatured polyacrylamide gel electrophoresis (dPAGE) before resuspension in PBS and storage at -80°C. T4 polynucleotide kinase (PNK), 10x PNK buffer, ATP solution, T4 DNA ligase, 10x ligase buffer, polyethylene glycol 4000 (PEG4000), dNTP mix, phi29 DNA polymerase, and 10x phi29 buffer were purchased from ThermoFisher Scientific. Quantifluor® ssDNA quantification system was purchased from Promega. Oligo(ethylene glycol) methyl ether methacrylate, M_n = 475 g/mol ($OEGMA_{475}$, 95%) was purchased from Sigma Aldrich and purified from added inhibitors hydroquinone monomethyl ether and butylated hydroxytoluene in a column of aluminum oxide (Sigma Aldrich, type CG-20). Silicone oil, Span® 80, Tween® 80, ethylene glycol dimethacrylate (EGDMA, 98%), ammonium persulfate (APS, 98%), magnesium sulfate ($MgSO_4$, >99.5%), and methacrylic acid (99%) were purchased from Sigma Aldrich and used as

received. Phosphate buffered saline (PBS), was purchased from Bioshop Canada Inc. at 10x liquid concentrate and diluted in Milli-Q grade distilled deionized water (DIW) as needed.

Table 3.1. Sequences of Oligonucleotides Utilized to Generate RCA Product and Detect DNA Hybridization

Oligonucleotide Abbreviation	Sequence (5' – 3')
CT	GAT CGT AGA CAA GAT GAT ACA GCA TTG AAG TCG AGG GTG TAT GAT GTG GTA AAG TAA GTG
LT	TT GTC TAC GAT CCA CTT ACT TT AC

3.2.2 Preparation of the circular DNA template

Circular DNA was synthesized via ligation of the ends of a linear, single stranded DNA sequence (CT, Table 2.1). To begin, the template was first phosphorylated at the 5' end by action of T4 PNK. 1000 pmol of linear precursor was mixed with 15 U of PNK and 1.5 mM of ATP in 1x PNK buffer (diluted from 10x in nuclease free water) to form a 100µL reaction mixture. The mixture was incubated at 37°C for 35 minutes and subsequently heated to 90°C for 5 minutes to denature the enzyme and terminate the reaction. Following phosphorylation, ligation was executed with T4 DNA ligase and a single stranded DNA sequence complementary to CT at the site of ligation (LT, Table 2.1). The 100µL PNK reaction mixture was first combined with 1100 pmol of LT, heated at 90°C for 1 minute and then cooled to room temperature for 20 minutes to promote strand annealing. Following cooling, 5 U of T4 DNA ligase and 30 µL of PEG4000 were added to the reaction. The final volume was brought to 300µL by addition of 30 µL of 10x T4 DNA ligase buffer and 124 µL of nuclease free water. The reaction was incubated at room temperature for 2 hours, after which the DNA was isolated by conventional ethanol precipitation. Circular DNA was separated from linear CT and LT by 10% dPAGE and quantified by measuring absorbance at 260 nm using the Tecan Infinite® M200 plate reader.

3.2.3 Synthesis of RCA product

Generation of RCA product was carried out by extending LT with free dNTP's using phi29 DNA polymerase in a 100µL reaction volume. Briefly, 28 pmol of circularized CT was mixed with 25 pmol of LT, 0.125 µmol of dNTP's and 25 U of phi29 DNA polymerase in 2.5x phi29 buffer (diluted from 10x in DIW). The reaction was incubated at 37°C for 1 hour, after which the product was heated at 90°C for 5 minutes to denature the enzyme. RCA product was purified from the reaction mixture in a 100 kDa Amicon® Ultra-0.5 mL centrifugal filter and resuspended in 100µL of 10 mM PBS. As CT was added in excess, it was assumed that the quantity of RCA product formed was equal to the amount of LT added (each product molecule extending from a single LT primer molecule), making the final concentration of RCA product 0.25 pmol/µL.

3.2.4 Polymerization of POEGMA microgels containing RCA product

POEGMA microgels were synthesized using an inverse water-in-oil (w/o) emulsion polymerization technique. For the optimized technique, 14 mL of 100 cSt silicone oil was mixed with 500 µL of emulsifiers composed of Span® 80 (85 v/v%) and Tween® 80 (15 v/v%) to create a continuous lipophilic phase containing 3.4 wt% emulsifiers. The oil phase was homogenized for 2 minutes at 5000 rpm before being placed in a 60°C oil bath and purged with nitrogen for 30 minutes under magnetic stirring at 1000 rpm. To prepare the hydrophilic phase, 1 mL of $OEGMA_{475}$, 400 µL of EDGMA, and 100 µL of RCA product were combined and gently mixed. The solution was added dropwise to the oil phase under magnetic stirring to yield a w/o emulsion consisting of 90 v/v% lipophilic and 10 v/v% hydrophilic phases. Following an additional 30 minutes, the polymerization reaction was started by injection of 0.16wt% of water-soluble initiator APS and left to stir for 15 minutes at 60°C under nitrogen. After the polymerization reaction was complete, particles were isolated by vacuum filtration with Whatman filter paper (grade 5, 2.5 µM

pore size), washed several times with DIW to remove lingering oils, and stored either in the dry state or in DIW at room temperature.

Several parameters in the above procedure were adjusted during optimization of the emulsion polymerization technique, including the viscosity of the silicone oil, the ratio of Span® 80/Tween® 80 in the emulsifiers, and the speed at which the mixture was agitated. Furthermore, attempts were made to electrostatically stabilize the particles by adding 1wt% $MgSO_4$, 3.1wt% of anionic aldehyde functionalized POEGMA (POA^-), or 0.31wt% of methacrylic acid to the water phase.

3.2.5 Characterization of microgel size

The relationship between average microgel diameter and key emulsion parameters was determined using a design of experiments (DOE) approach. A full factorial design was set up to determine the influence of emulsifier concentration, initiator concentration, and temperature of the reaction on the average microgel size. The high and low levels of each factor are summarized in Table 3.2, and the order of the experiments is summarized in Table 3.3. Polymerizations were carried out with all other conditions remaining constant at the specifications described in section 3.2.4. Following rinsing, particles were resuspended in DIW and imaged on an inverted brightfield microscope. Photos were analyzed using the ImageJ particle analysis tool to determine an average particle size. A total of six photos were taken for each experiment, three at 4x magnification and three at 10x magnification. Averages from each magnification were taken (n=3) and utilized as data points in the factorial design, such that two diameters were reported for each experiment; this yielded 8 degrees of freedom when fitting the model. The data was analyzed in R software to establish a linear predictive model of diameter based on the emulsion parameters.

Table 3.2. Low and High Levels of Emulsifier, Initiator, and Temperature in the Full Factorial

Factor	Low (-)	High (+)
Emulsifier Concentration	1.3wt%	4.9wt%
Initiator Concentration	0.125wt%	0.195wt%
Temperature	60°C	80°C

Table 3.3. Full Factorial Experimental Design

Standard Order	Actual Order	Emulsifier	Initiator	Temperature
1	4	-	-	-
2	1	+	-	-
3	5	-	+	-
4	8	+	+	-
5	3	-	-	+
6	2	+	-	+
7	6	-	+	+
8	7	+	+	+

3.2.6 Encapsulation efficiency of RCA product

RCA product was synthesized as per section 3.2.3 and quantified with Quantifluor® ssDNA dye according to the manufacturer's instructions (Quantifluor® ssDNA System, Product E3190 Quick Protocol, Promega) using the Multiwell Plate Protocol and the high concentration standard curve (Figure A.1). 100 µL of RCA product was added to the water phase, and microgels were synthesized as reported in section 3.2.4. Following isolation and drying of the particles, 10 mg of particles were weighed and combined with Quantifluor® ssDNA working solution to identify the mass of DNA per milligram of microparticles, utilizing the low concentration standard curve generated with a TECAN M1000 plate reader (Figure A.2). The total amount of RCA product in the microparticles was determined by multiplying this value by the total mass of particles isolated and subsequently dividing by the original mass of RCA product added to the water phase to determine the encapsulation efficiency (% of RCA product entrapped in the microgels).

3.3 Results and Discussion

3.3.1 Optimization of POEGMA Microgel Synthesis

Preliminary polymerization experiments followed a modified procedure from Kriwet et al. and resulted in large, highly disperse and ill-structured microgels.[56] Briefly, a mixture of 14 mL of 5 cSt silicone oil and 500µL (3.4 wt%) of a 75:25 mixture of Span®80 and Tween®80 was vortexed and purged with nitrogen before dropwise addition of hydrophilic phase (1 mL $OEGMA_{475}$, 400 µL EDGMA). Following an additional 30 minutes of purging, water soluble initiator (APS, 0.16wt%) was added to the vessel, and the reaction was allowed to proceed under 400 rpm mechanical stirring for 2 hours at 60°C. The resultant microgels are shown in Figure 3.1. Kriwet et al. reported the polymerization of both micro and nano-sized particles of polyacrylic acid, with microgels evolving from the use of water-soluble initiator (APS) and nanogels arising when polymerization was initiated by the oil-soluble initiator azo-bis-isobutyronitrile (AIBN).[56] With the anticipated end use of POEGMA microgels as the ligand support in affinity columns, APS was selected as the initiator of choice to keep particles at a large enough size (~30-50 µm diameter) such that the pressure drop across the column is limited.

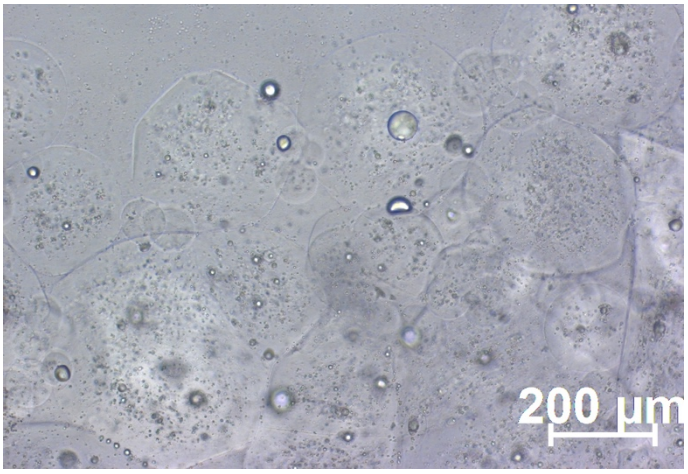

Figure 3.1 Microgels synthesized following a modified procedure from Kriwet et al.[56]

It is evident from Figure 3.1 that the obtained particles are far from ideal, with significant aggregation of particles and an average diameter (244 ± 39 μm) considerably larger than the specified goal. In an initial attempt of mitigating this without striving too far from the established method in the literature, the viscosity of silicone oil was shifted to 50 and 100 cSt. According to Alvarado et al., the viscosity of the continuous phase has significant influence on the stability of w/o emulsions, with higher viscosities imparting a greater resistance to droplet coalescence and phase separation;[59] additionally, Anisa and Nour demonstrated that higher viscosity oils contributed to lower average droplet sizes for w/o emulsions.[96] As such, there are multiple predicted benefits of increasing the continuous phase viscosity. Figure 3.2 demonstrates typical images taken from emulsions prepared at higher continuous phase viscosities. Not only did the particle size decrease significantly, (57 ± 11 μm and 53 ± 7 μm diameter for 50 cSt and 100 cSt, respectively) but the distribution of particle sizes produced also became much smaller. It should be noted that there was no noticeable difference in emulsions prepared in 50 cSt relative to 100 cSt oil, which suggests an upper ceiling for the influence of viscosity beyond which no greater stability is conferred. This phenomenon has previously been described in oil-in-water emulsions, with the difference in viscosity between the phases influencing stability and size up to some critical ratio beyond which no changes to droplet diameter were noted.[97]

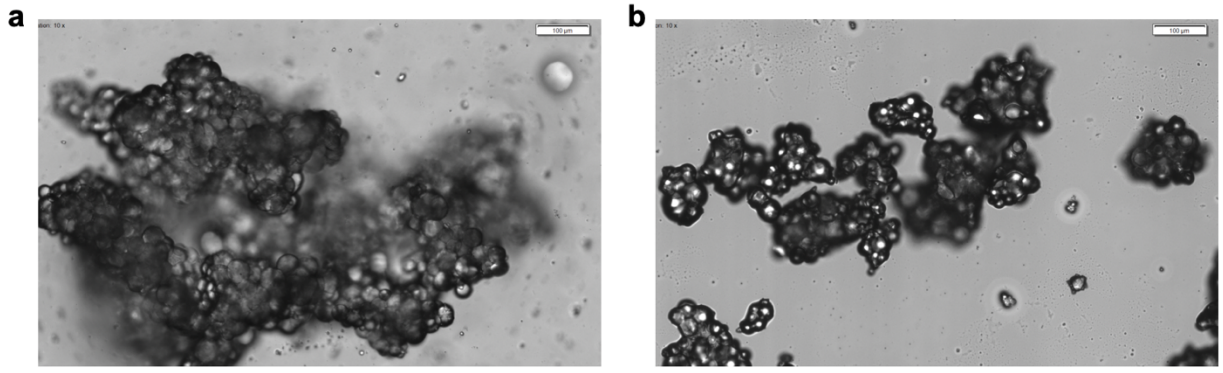

Figure 3.2. Microgels synthesized in **(a)** 50 cSt silicone oil and **(b)** 100 cSt silicone oil. Scale bars represent 100 μm.

Following the adjustment to viscosity, it became obvious that coagulation of particles was a major issue, with microgels coalescing during polymerization and rapidly settling in solution. To resolve this problem, the volume ratio of Span® 80/Tween® 80 was adjusted from the original 75:25 mixture. ICI Americas introduced a systematic method for quantifying emulsifier suitability by assigning each emulsifier a numerical value for its hydrophilic-lipophilic balance (HLB), the balance of the length and power of the hydrophilic and lipophilic groups in the emulsifier.[57] Those with more lipophilic character are assigned low HLB values (i.e. Span® 80, HLB = 4.3), while those with more hydrophilic character have higher values (i.e. Tween® 80, HLB = 15). The HLB value of emulsifier blends can be calculated by a simple weighted average. In w/o emulsions, it is recommended that the emulsifier blend have an HLB between 4-6, as oil-soluble emulsifiers yield stable w/o emulsions.[57] Furthermore, individual oils will have a "required HLB", with the suggested HLB for silicone oil being 6. Based on this recommendation, the ideal emulsifier ratio was calculated to be 85:15 Span® 80/Tween® 80, yielding an HLB of 5.91.

Different blends of Span® 80/Tween® 80 were tried and added to the silicone oil at 3.4 wt% of the lipophilic phase (3.1 wt% of the total mixture), and the resultant particles are depicted in Figure 3.3. Although some aggregation of particles is still present, the borders of individual microgels become substantially more defined with an increasing ratio of Span® 80/Tween® 80. Due to the improvement noted, the procedure was adjusted to include an 85:15 Span® 80/Tween® 80 ratio of emulsifiers.

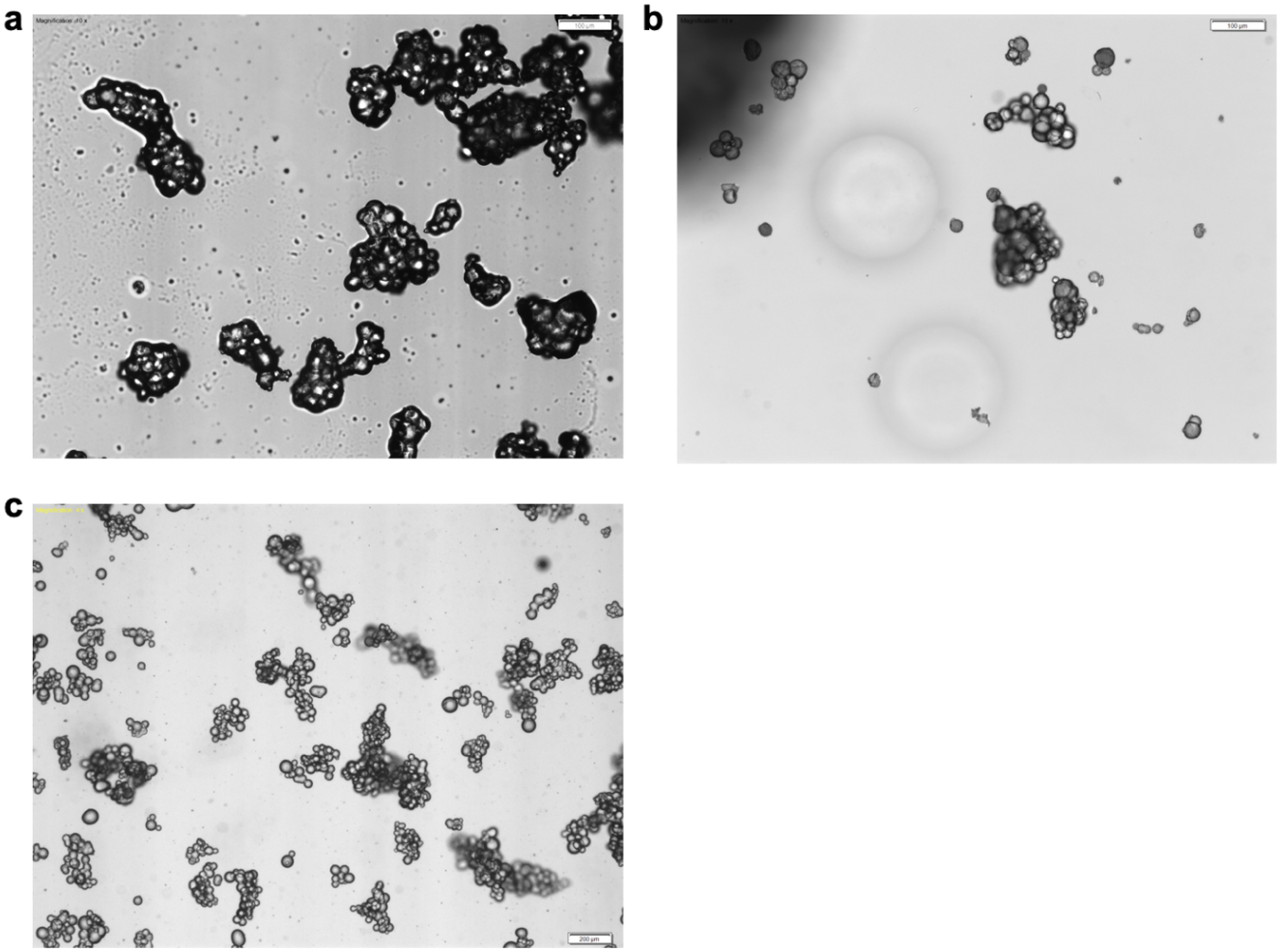

Figure 3.3. Microgels synthesized with different emulsifier mixtures at 3.4wt% in 100 cSt silicon oil **(a)** 70:30 Span® 80/Tween® 80, **(b)** 80:20 Span® 80/Tween® 80, **(c)** 85:15 Span® 80/Tween® 80. Scale bars represent 100 µm (a and b) and 200 µm (c).

Different electrostatic stabilizers were then tested to further reduce particle aggregation during the polymerization process; however none were particularly effective. Firstly, $MgSO_4$ was added to the water phase at 1wt% in accordance with dual reports from Kent and Saunders and Aronson and Petko that demonstrated stability against droplet coalescence with the addition of electrolytes to the water phase.[98, 99] In another experiment, methacrylic acid was added to the water phase with the notion that introducing a net negative charge to the droplets would induce electrostatic repulsion that would hinder particle fusion. However, the trial proved unsuccessful,

likely attributed to the low electrical conductivity of the oil phase that renders electrostatic stabilization techniques futile. To induce a larger net negative charge and sterically obstruct particle coagulation, POA^- was added to the water phase, however its incorporation also had little effect. Representative images from these stabilization studies are demonstrated in Figure 3.4.

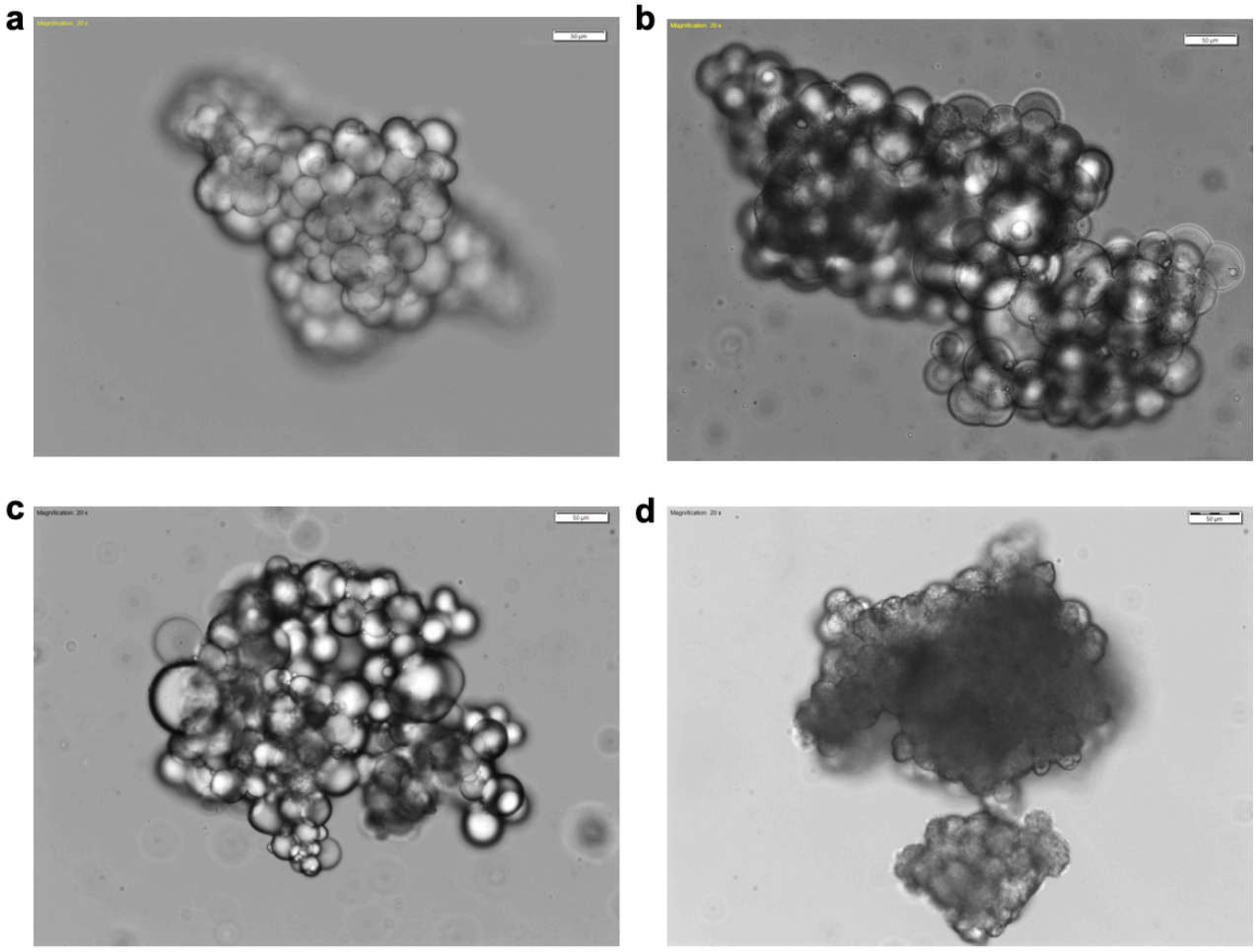

Figure 3.4. Microgels synthesized with different electrostatic stabilizers in the hydrophilic phase **(a)** no electrostatic stabilizers, **(b)** 1wt% $MgSO_4$, **(c)** 0.09wt% Methacrylic Acid, **(d)** 3.1wt% of anionic POA. Scale bars represent 50 µm.

With electrostatic stabilization yielding unsatisfactory results, the energy of mixing was increased by homogenizing the oil and emulsifiers at 5000 rpm for 2 minutes prior to polymerization. The magnetic stir speed was also increased from 400 rpm to 1000 rpm throughout

the polymerization to maintain a greater shear stress and reduce the tendency for coalescence. Emulsification is a non-spontaneous process, with water droplets preferentially combining to achieve a smaller interfacial area with the oil phase. To provide the free energy necessary to overcome the positive Gibb's free energy change accompanied by emulsification, mechanical shearing by mixing is typically used as a source of energy. Theoretically, higher stir speeds should contribute to a greater input energy and thus more resistance to particle coalescence. The combined efforts of homogenization and more rigorous magnetic stirring led to an emulsion with improved stability, with noticeably fewer aggregates as demonstrated in Figure 3.5. Following this discovery, the polymerization procedure was adjusted to reflect the changes made in this study.

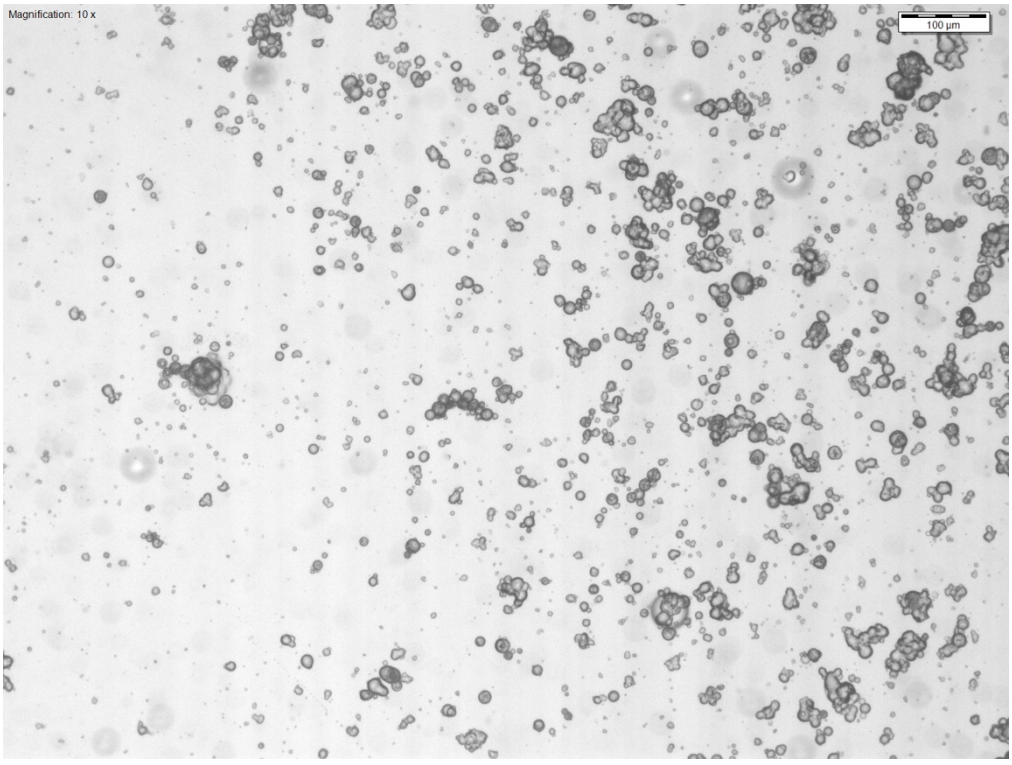

Figure 3.5. Microgels synthesized under 1000 rpm mechanical stirring with a liphophilic phase subject to homogenization at 5000 rpm for 2 minutes prior to starting the polymerization. Scale bar represents 200 µm.

3.3.2 Factors influencing average microgel size

Analysis of the full factorial DOE reveal that both emulsifier and initiator concentration have an inverse influence on microgel size, while temperature has a negligible effect. The magnitude of the effect of all tested factors and their interactions is summarized in Figure 3.6, with error bars representing a 95% confidence interval on 8 degrees of freedom. The plot reinforces the significance of emulsifier and initiator concentration, as the confidence intervals do not span 0 (signifying that there is a unidirectional effect of these factors on microgel size). The opposite can be said for temperature and all two-parameter interactions, as none of these parameters are significant at the 95% confidence interval. From this analysis, a linear predictive model was developed for microgel diameter and is summarized in equation 3.1, where (emulsifier) and (initiator) are in coded units.

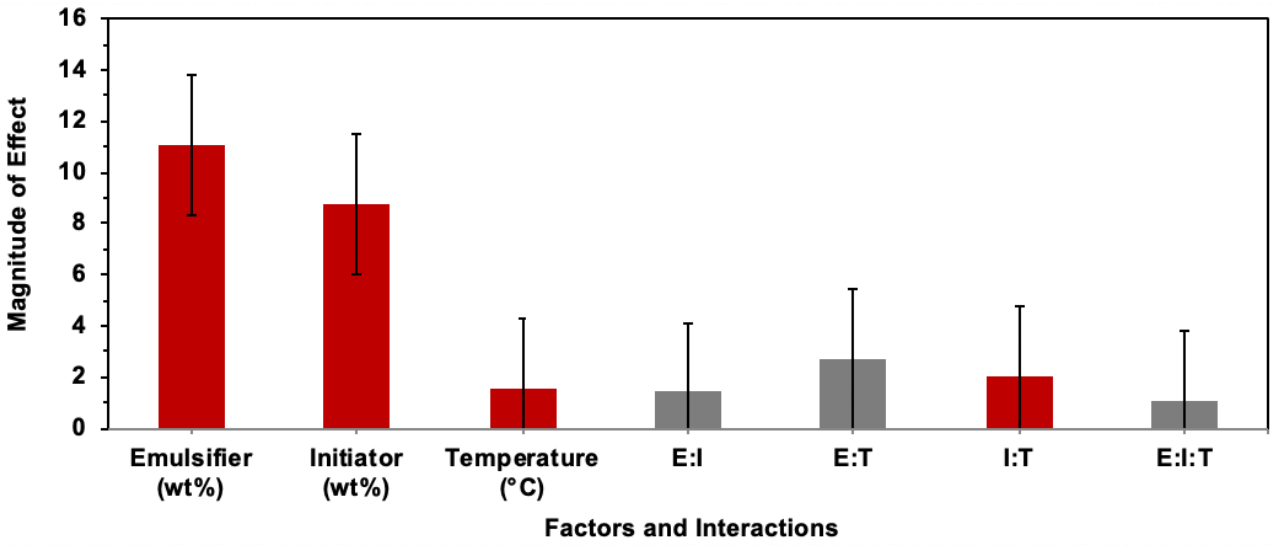

Figure 3.6. Estimated coefficients for the influence of factors and interactions on microgel diameter, (■) denoting positive relationships and (■) signifying negative relationships. Error bars represent the 95% confidence interval for each coefficient.

$$\textbf{Microgel Diameter} = 27.698 - 11.110(\textbf{Emulsifier}) - 8.758(\textbf{Initiator}) \qquad \textbf{(3.1)}$$

The linear model in equation 3.1 was used to predict the size of different microgels to evaluate the suitability of the model. Figure 3.7 demonstrates the actual vs predicted microgel size, with the line of equality plotted as a point of reference. It is evident that the model accurately predicts the size at the 95% confidence interval over a broad range of sizes (10-60 μm), with data falling along the line of ideality. Following confirmation of its predictive capacity, the model was converted to actual units with (emulsifier) and (initiator) in wt%. The modified model is presented in Equation 3.2. It should be noted, however, that no microgels can be synthesized with 0wt% of either initiator or emulsifier as both are needed to initiate and stabilize polymer formation. The lower bounds at which this equation is valid are at 0.7wt% of emulsifier and 0.09wt% of initiator, as successful microgels were generated at these concentrations, and the predictive nature of the model remained valid within this range.

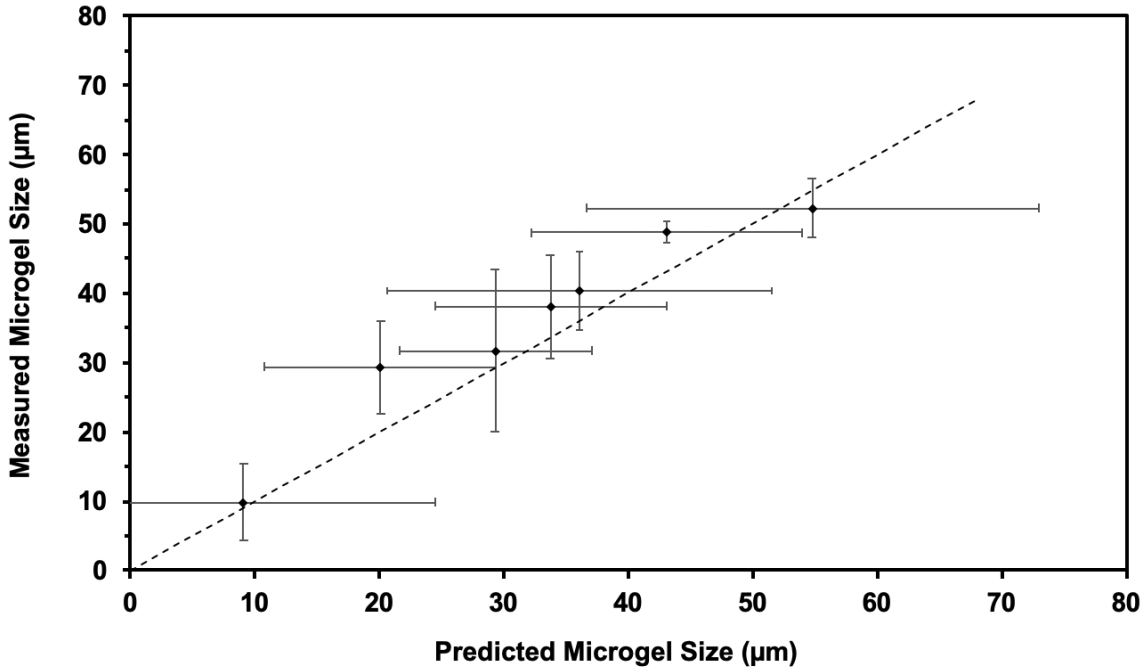

Figure 3.7 Actual microgel diameters as determined from ImageJ software plotted against the sizes predicted from the linear model in equation 3.1. Horizontal error bars represent the 95% confidence interval on the predicted size, vertical error bars are ± 1 s.d., and the dashed line denotes the ideal outcome wherein actual = predicted diameter.

$$\textbf{Microgel Diameter} = 86.251 - 6.172(\textbf{Emulsifier}) - 250.229(\textbf{Initiator}) \quad \textbf{(3.2)}$$

The inverse relationships between emulsifier and initiator concentration and size are not particularly surprising. Kireev et al. showed similar trends with polymerization of polyvinyl alcohol, namely a larger average particle size with lower added initiator and stabilizers.[58] Kurenkov et al. also reported lower molecular weight particles at higher concentrations of both emulsifier and initiator.[100] What is more surprising is the negligible influence of temperature on the particle size, as it was expected that an elevated temperature would lead to smaller particles due to an increase in termination and chain transfer rate.[60] However, higher temperatures could also contribute to more molecular motion and diffusion of monomer to sites of polymerization, contributing to larger average particle sizes. Therefore, it is possible that the lack of influence on microgel size is due to the rival effects that temperature has on the progression of polymerization.

Figure 3.8 displays representative figures from the experiment with the lowest concentration of initiator and emulsifier in comparison with the highest values of both parameters. It can be noted that as microgel size gets smaller (from Figure 3.8 (a) to 3.8 (b)), the tendency for coagulation becomes far more pronounced, likely due to the higher interfacial free energy present with smaller particles that could not be mitigated by the higher energy input. Particle aggregation at higher emulsifier concentrations negates some of the recommendations identified during optimization of the polymerization procedure, with several sources reporting 10wt% emulsifiers as the ideal concentration to generate stable emulsions.[101] This illuminates the inherent difficulty in perfecting an emulsion polymerization procedure; although some general trends reported in the literature will hold, each system is incredibly unique and requires precise tuning of parameters to reach a formulation that works for the particular system. Thus, the technique reported and model

for size prediction generated here are both relevant only to the polymerization of POEGMA microgels in silicone oil and cannot be generalized for other systems.

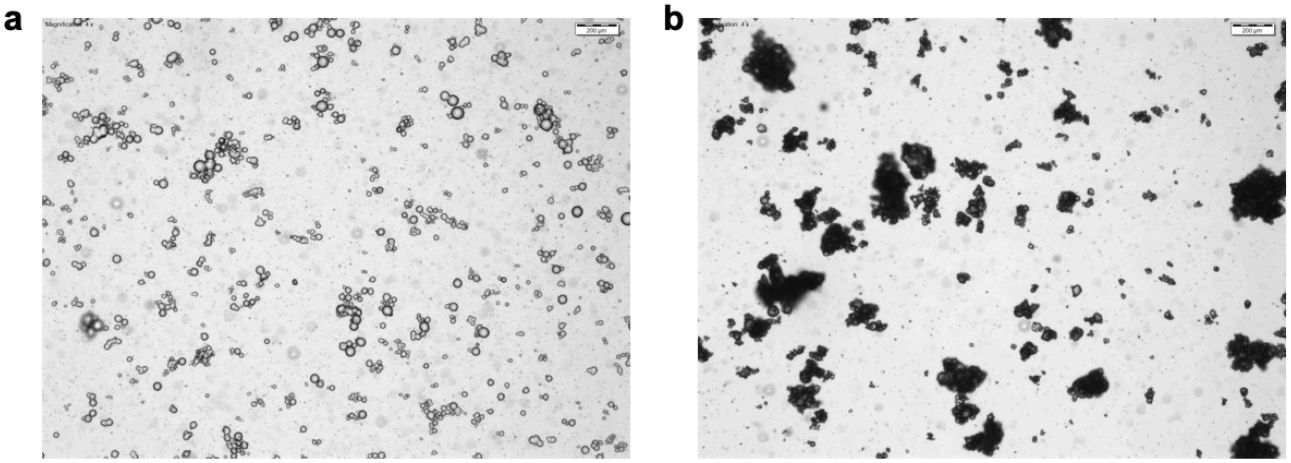

Figure 3.8. Microgels synthesized with **(a)** 4.9wt% emulsifier and 0.195wt% initiator and **(b)** 1.3wt% of emulsifier and 0.125wt% of initiator.

3.3.3 Encapsulation Efficiency of RCA product in POEGMA microgels

The percentage of entrapped RCA product was calculated for microgels of different sizes, with larger microgels encapsulating a greater fraction of RCA product and 50 µm particles encapsulating a maximum of 56% of the original DNA. Figure 3.9 demonstrates the relationship between microgel diameter and encapsulation efficiency, with sizes determined using ImageJ software. It is clearly evident that larger particles encapsulate a higher amount of DNA, with 10 µm sized particles entrapping a nearly negligible amount of RCA product. This relationship can likely be attributed to the system's entropic drive to achieve thermodynamic equilibrium. Although the polarity of DNA renders it hydrophilic, such that it preferentially partitions in the water phase, it is possible that as the aqueous droplets shrink in size the repulsion of the negative DNA and tendency for the molecule to spread dominates. Thus, in smaller microgels it may be

thermodynamically favourable for the RCA product to separate into the oil phase, contributing to a lower encapsulation efficiency in smaller particles.

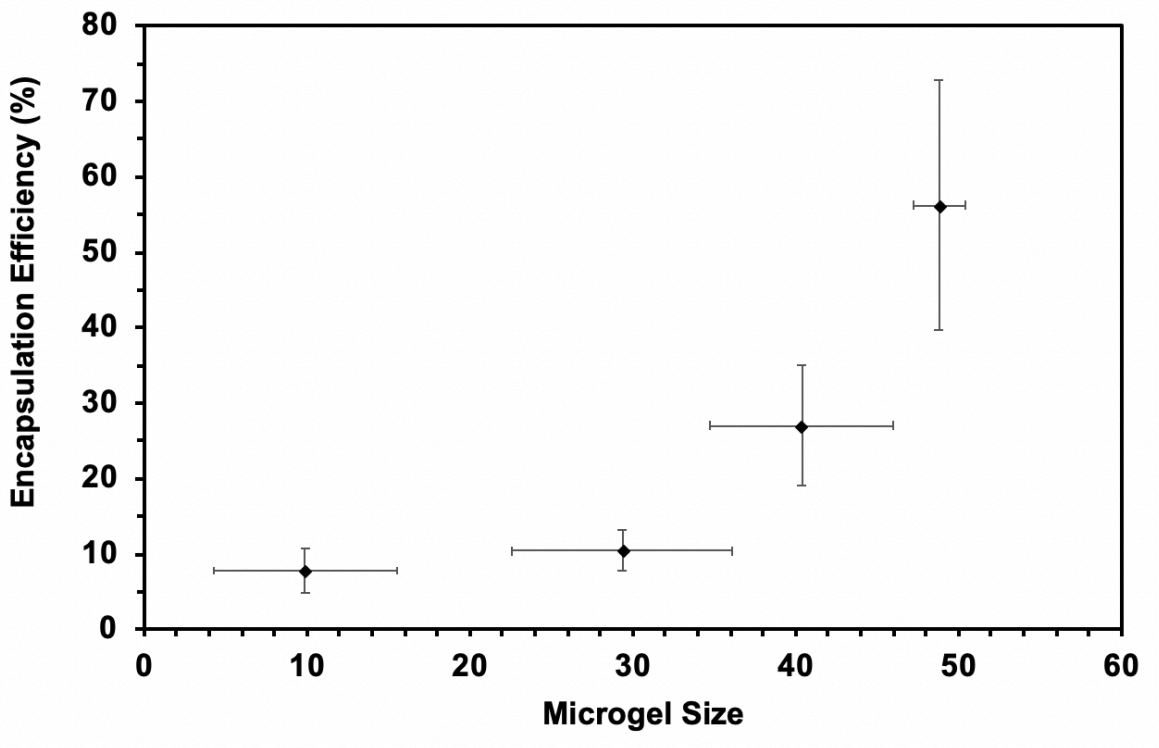

Figure 3.9 Encapsulation efficiency (%) of RCA product within different sized POEGMA microgels. Data are means ± 1 s.d (n = 3).

`

It should be noted that in a quest to determine the encapsulation efficiency of the RCA product, 100 µL of 20 base pair fluorescein-labeled DNA probe (FP) was added to the water phase to visualize whether DNA could partition into the aqueous phase and remain within the gels following polymerization. Figure 3.10 shows a fluorescent image of microgels containing FP in comparison with gels synthesized without the presence of DNA, visually demonstrating that DNA can be incorporated into the POEGMA microgels. The encapsulation efficiency of FP was calculated using a similar procedure to 3.2.6; however, concentrations of DNA were determined from the fluorescence of FP (standard curve presented in Figure A.3) as opposed to staining with the Quantifluor® ssDNA dye. The encapsulation efficiency of FP was 21 ± 1% in microparticles

synthesized as described in section 3.2.4 (estimated size of 29 μm). This is comparable to the encapsulation efficiency of RCA product in similarly sized microgels (Figure 3.9), suggesting significant hindrance to probe diffusion out of the microgels. To test this theory, microgels with a lower crosslinking density (prepared by adding only 40 μL of the EDGMA crosslinker) were synthesized and displayed an encapsulation efficiency of merely 1.9 ± 0.3%, potentially due to diffusion of the incorporated probe out of the microgels during storage in fresh DIW. This result implies that the amount of crosslinker added has an influence on the ability for small targets to diffuse through the gel. Moving forward, it would be beneficial to study RCA product within lower crosslinked microgels, as ease of diffusion of targets to the interior of the gel is necessary in the pursuit of a high binding capacity.

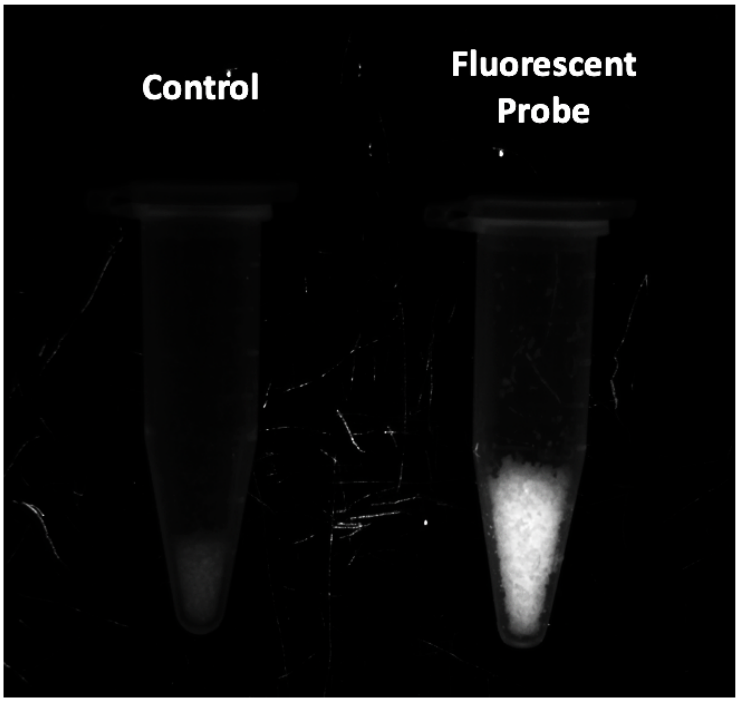

Figure 3.10. Fluorescence of POEGMA microparticles alone (control) in comparison to POEGMA microparticles synthesized with FP in the aqueous phase.

3.4 Conclusion

POEGMA microgels containing RCA product were successfully synthesized utilizing an inverse emulsion polymerization technique. An optimized polymerization procedure that mitigated particle aggregation by increasing the viscosity of the continuous phase, the ratio of Span® 80 to Tween® 80, and the energy of mixing via homogenization and magnetic stir speed was reported. A linear predictive model for the microgel size based on the concentration of initiator and emulsifier was developed using a design of experiments approach, with accurate predictions for diameter achieved 95% confidence over a broad range of sizes. RCA product was encapsulated in microgels of different sizes, with larger particles incorporating higher amounts of DNA and 50 μm gels yielding the greatest encapsulation efficiency at 56% of the original mass of RCA product. Moving forward, analysis of the orientation of RCA product within the hydrogel particles would be of interest, specifically what fraction of RCA product is buried within the hydrogel network (versus protruded from the gel) and whether or not it is possible to tune the accessibility of various probes in and out of the microgel network by adjusting the polymerization procedure. Additionally, the stability of the RCA product/POEGMA gels in different hostile environments (nucleases, basic conditions) is vital to determine the longevity of the system and the protective effect the hydrogel has on the fragile encapsulated DNA chain. Finally, it would be beneficial to load a column with POEGMA/RCA product microparticles and probe the ability of the system to preferentially capture complementary DNA targets from a continuous flow sample, relevant for identifying end applications of this novel material.

Chapter 4: Conclusions and Recommendations

4.1 Summary of Work

POEGMA hydrogels were utilized to stabilize RCA product in two different assemblies: thin film microarrays formulated by BioJet printing and spherical microgels synthesized by inverse emulsion polymerization. First, microarrays were developed by printing aldehyde followed by hydrazide functionalized POEGMA precursors along with RCA product onto a nitrocellulose substrate. The printer was able to evenly and consistently distribute RCA product in all microzones, with a coefficient of variation as low as 5.5% indicating the suitability of this platform for microarray biosensing. Moreover, the thin polymeric film that formed as the result of hydrazone crosslinking was able to immobilize and protect the RCA product from several cycles of washing in salt and detergents. Introduction of complementary DNA probe to the system to assess the potential for hybridization of target molecules proved challenging, with a signal to noise ratio close to 1 for the base formulation as well as many other compositional iterations. Centrifugation and sonication of the substrate did not dislodge the probe from the hydrogel network. Application of an electric field successfully dislodged the probe from the negative controls, at which point the hybridization conditions and polymer charge were adjusted to optimize strand annealing and electrostatically repel the probe from being trapped in the polymer network. Upon changes to the hybridization buffer and time, the signal to noise ratio was improved to ~4 over a large range of probe concentrations. Introducing both positive and negative charges to the hydrogel system had similar effects, maintaining the higher signal to noise ratio even at lower concentrations of probe.

Second, POEGMA microgels were fabricated by emulsifying monomer and crosslinker in silicone oil using a combination of Span®80 and Tween®80 and subsequently initiating free radical

polymerization with water-soluble APS. The polymerization procedure was optimized to generate particles stable against coalescence by increasing the oil phase viscosity, the ratio of Span®80 to Tween®80 in the emulsifiers, and the mechanical shearing during polymerization. Furthermore, a linear predictive model of microgel diameter as a function of the initiator and emulsifier concentrations was developed and could accurately predict microgel sizes in the range of 10-60 μm. Finally, RCA product was successfully incorporated into POEGMA microgels, with larger gels encapsulating a greater fraction of the added DNA up to the highest reported encapsulation of 56% achieved with 50 μm particles.

4.2 Future Directions

The primary goal of this thesis was achieved, with two different POEGMA hydrogel systems successfully synthesized with RCA product physically entrapped. However, much of the work done thus far was related to the development and characterization of this new material combination. There is still much work that needs to be done in order to explore the potential applications of this novel system.

It would be beneficial to increase the signal to noise ratio in the DNA microarrays even further, to avoid errors or false positives in sensing generated from non-specific binding. Of particular interest is the hybridization of complementary probe to RCA product encapsulated within negatively charged polymer systems at temperatures above the VPTT of the hydrogel. Hybridization is most efficient at a temperature ~20°C below the melting temperature of annealed DNA strands, calculated to be 64°C for the sequences used in this study. However, with the hydrogel used in this work collapsing above ~33°C (the VPTT), RCA product buried within the hydrogel becomes inaccessible to the oligonucleotide. With that said, it is possible that the negative charge on the anionic POEGMA system repels the RCA product to the surface of the gel,

increasing the accessibility of binding sites at temperatures above the VPTT in comparison to neutral polymer systems. This theory could be confirmed by hybridizing complementary probe to RCA within anionic POEGMA at 44°C, to assess if an increased signal to noise ratio is identified.

It would also be desirable to gain a better understanding of the orientation of RCA product within both hydrogel systems by fluorescently labeling polymer precursors and DNA with different fluorophores and imaging the gels on a confocal microscope. The accessibility of the RCA product – namely, does it protrude from the gel or is it entirely encased within the polymer – would be useful in determining whether diffusion of targets to the interior of the gels is a major concern. Perhaps a significant portion of the RCA product is extending from the gel, such that the hydrogels can be made even more dense to stop non-specific absorption of targets to the interior of the gel without compromising the potential for hybridization events to occur.

Finally, experiments probing the end use of these systems are valuable for reporting the potential applications of these materials. Introducing a variety of different DNA targets to the microarray system and investigating whether the microzones containing RCA product can preferentially retain complementary oligos is of interest. Additionally, it would be fascinating to load a flow through column with POEGMA microgels and introduce a mixture of low concentration oligos to the mobile phase to see if particles containing RCA product can favourably capture complementary probe and later elute and quantify them at higher concentrations.

While there is still room to explore this system and determine potential end use applications, the work done here has demonstrated that the encapsulation of RCA product within POEGMA hydrogels is feasible, providing a basis for the further development of a novel biosensing material.

References

[1] S. H. Gellman, "Introduction: molecular recognition," ed: ACS Publications, 1997.

[2] F. Scheller *et al.*, "Research and development of biosensors. A review," *Analyst,* vol. 114, no. 6, pp. 653-662, 1989.

[3] D. J. Claremont, G. W. Shaw, and J. C. Pickup, "Biosensors for continuous in vivo glucose monitoring," in *Proceedings of the Annual International Conference of the IEEE Engineering in Medicine and Biology Society*, 1988: IEEE, pp. 740-741.

[4] P. B. Luppa, C. Müller, A. Schlichtiger, and H. Schlebusch, "Point-of-care testing (POCT): Current techniques and future perspectives," *TrAC Trends in Analytical Chemistry,* vol. 30, no. 6, pp. 887-898, 2011.

[5] B. B. Rodriguez, J. A. Bolbot, and I. E. Tothill, "Urease–glutamic dehydrogenase biosensor for screening heavy metals in water and soil samples," *Analytical and bioanalytical chemistry,* vol. 380, no. 2, pp. 284-292, 2004.

[6] T. Montesinos, S. Pérez-Munguia, F. Valdez, and J.-L. Marty, "Disposable cholinesterase biosensor for the detection of pesticides in water-miscible organic solvents," *Analytica Chimica Acta,* vol. 431, no. 2, pp. 231-237, 2001.

[7] N. Mungroo and S. Neethirajan, "Biosensors for the detection of antibiotics in poultry industry—a review," *Biosensors,* vol. 4, no. 4, pp. 472-493, 2014.

[8] S. Song, L. Wang, J. Li, C. Fan, and J. Zhao, "Aptamer-based biosensors," *TrAC Trends in Analytical Chemistry,* vol. 27, no. 2, pp. 108-117, 2008.

[9] C. Tuerk and L. Gold, "Systematic evolution of ligands by exponential enrichment: RNA ligands to bacteriophage T4 DNA polymerase," *Science,* vol. 249, no. 4968, pp. 505-510, 1990.

[10] A. D. Ellington and J. W. Szostak, "Selection in vitro of single-stranded DNA molecules that fold into specific ligand-binding structures," *Nature,* vol. 355, no. 6363, p. 850, 1992.

[11] C. Kessler, "Overview on factors influencing nucleic acid hybridization," in *Nonradioactive Analysis of Biomolecules*: Springer, 2000, pp. 437-442.

[12] M. Minuth. (2013). *Stronger base pairing improves DNA analysis* [Online]. Available: https://www.gesundheitsindustrie-bw.de/en/article/news/stronger-base-pairing-improves-dna-analyses/.

[13] O. Wolter and G. Mayer, "Aptamers as valuable molecular tools in neurosciences," *Journal of Neuroscience,* vol. 37, no. 10, pp. 2517-2523, 2017.

[14] M. Schena, D. Shalon, R. W. Davis, and P. O. Brown, "Quantitative monitoring of gene expression patterns with a complementary DNA microarray," *Science,* vol. 270, no. 5235, pp. 467-470, 1995.

[15] S. M. Yoo, J. H. Choi, S. Lee, N. C. Yoo, J. Choi, and N. Yoo, "Applications of DNA microarray in disease diagnostics," *Journal of microbiology and biotechnology,* vol. 19, no. 7, pp. 635-646, 2009.

[16] N. L. van Hal *et al.*, "The application of DNA microarrays in gene expression analysis," *Journal of biotechnology,* vol. 78, no. 3, pp. 271-280, 2000.

[17] F. Teletchea, J. Bernillon, M. Duffraisse, V. Laudet, and C. Hänni, "Molecular identification of vertebrate species by oligonucleotide microarray in food and forensic samples," *Journal of Applied Ecology,* vol. 45, no. 3, pp. 967-975, 2008.

[18] I. Y. Jung, J. S. Kim, B. R. Choi, K. Lee, and H. Lee, "Hydrogel based biosensors for in vitro diagnostics of biochemicals, proteins, and genes," *Advanced healthcare materials,* vol. 6, no. 12, p. 1601475, 2017.
[19] D. From, "biosensors to gene chips Wang, Joseph," *Nucleic Acids Research,* vol. 28, no. 16, pp. 3011-3016, 2000.
[20] S. Draghici, P. Khatri, A. C. Eklund, and Z. Szallasi, "Reliability and reproducibility issues in DNA microarray measurements," *TRENDS in Genetics,* vol. 22, no. 2, pp. 101-109, 2006.
[21] G. Cohen, J. Deutsch, J. Fineberg, and A. Levine, "Covalent attachment of DNA oligonucleotides to glass," *Nucleic acids research,* vol. 25, no. 4, pp. 911-912, 1997.
[22] M. Hegner, P. Wagner, and G. Semenza, "Immobilizing DNA on gold via thiol modification for atomic force microscopy imaging in buffer solutions," *FEBS letters,* vol. 336, no. 3, pp. 452-456, 1993.
[23] C. Larsson, M. Rodahl, and F. Höök, "Characterization of DNA immobilization and subsequent hybridization on a 2D arrangement of streptavidin on a biotin-modified lipid bilayer supported on SiO2," *Analytical Chemistry,* vol. 75, no. 19, pp. 5080-5087, 2003.
[24] X. Zhao and J. K. Johnson, "Simulation of adsorption of DNA on carbon nanotubes," *Journal of the American Chemical Society,* vol. 129, no. 34, pp. 10438-10445, 2007.
[25] I. Barbulovic-Nad, M. Lucente, Y. Sun, M. Zhang, A. R. Wheeler, and M. Bussmann, "Bio-microarray fabrication techniques—a review," *Critical reviews in biotechnology,* vol. 26, no. 4, pp. 237-259, 2006.
[26] F. Xu, A. M. Pellino, and W. Knoll, "Electrostatic repulsion and steric hindrance effects of surface probe density on deoxyribonucleic acid (DNA)/peptide nucleic acid (PNA) hybridization," *Thin Solid Films,* vol. 516, no. 23, pp. 8634-8639, 2008.
[27] V. Chan, D. J. Graves, and S. E. McKenzie, "The biophysics of DNA hybridization with immobilized oligonucleotide probes," *Biophysical journal,* vol. 69, no. 6, pp. 2243-2255, 1995.
[28] C. Katevatis, A. Fan, and C. M. Klapperich, "Low concentration DNA extraction and recovery using a silica solid phase," *PloS one,* vol. 12, no. 5, p. e0176848, 2017.
[29] D. Liu *et al.*, "Gold nanoparticle-based activatable probe for sensing ultralow levels of prostate-specific antigen," *ACS nano,* vol. 7, no. 6, pp. 5568-5576, 2013.
[30] A. Umar, M. Rahman, M. Vaseem, and Y.-B. Hahn, "Ultra-sensitive cholesterol biosensor based on low-temperature grown ZnO nanoparticles," *Electrochemistry Communications,* vol. 11, no. 1, pp. 118-121, 2009.
[31] M. Lee and D. R. Walt, "A fiber-optic microarray biosensor using aptamers as receptors," *Analytical Biochemistry,* vol. 282, no. 1, pp. 142-146, 2000.
[32] Q. Zhao, X.-F. Li, Y. Shao, and X. C. Le, "Aptamer-based affinity chromatographic assays for thrombin," *Analytical chemistry,* vol. 80, no. 19, pp. 7586-7593, 2008.
[33] G. A. Zelada-Guillén, J. Riu, A. Düzgün, and F. X. Rius, "Immediate detection of living bacteria at ultralow concentrations using a carbon nanotube based potentiometric aptasensor," *Angewandte chemie international edition,* vol. 48, no. 40, pp. 7334-7337, 2009.
[34] O. Okay, "General properties of hydrogels," in *Hydrogel sensors and actuators*: Springer, 2009, pp. 1-14.
[35] A. S. Hoffman, "Hydrogels for biomedical applications," *Advanced drug delivery reviews,* vol. 64, pp. 18-23, 2012.

[36] J. Tavakoli and Y. Tang, "Hydrogel based sensors for biomedical applications: An updated review," *Polymers,* vol. 9, no. 8, p. 364, 2017.
[37] D. Proudnikov, E. Timofeev, and A. Mirzabekov, "Immobilization of DNA in polyacrylamide gel for the manufacture of DNA and DNA–oligonucleotide microchips," *Analytical biochemistry,* vol. 259, no. 1, pp. 34-41, 1998.
[38] S. Brahim, D. Narinesingh, and A. Guiseppi-Elie, "Bio-smart hydrogels: co-joined molecular recognition and signal transduction in biosensor fabrication and drug delivery," *Biosensors and Bioelectronics,* vol. 17, no. 11-12, pp. 973-981, 2002.
[39] N. Sorokin, V. Chechetkin, M. Livshits, V. Vasiliskov, A. Turygin, and A. Mirzabekov, "Kinetics of hybridization on the oligonucleotide microchips with gel pads," *Journal of Biomolecular Structure and Dynamics,* vol. 21, no. 2, pp. 279-288, 2003.
[40] A. Beyer, S. Pollok, A. Berg, K. Weber, and J. Popp, "Easy daylight fabricated hydrogel array for colorimetric DNA analysis," *Macromolecular bioscience,* vol. 14, no. 6, pp. 889-898, 2014.
[41] A. Baeissa, N. Dave, B. D. Smith, and J. Liu, "DNA-functionalized monolithic hydrogels and gold nanoparticles for colorimetric DNA detection," *ACS applied materials & interfaces,* vol. 2, no. 12, pp. 3594-3600, 2010.
[42] R. L. Srinivas, S. C. Chapin, and P. S. Doyle, "Aptamer-functionalized microgel particles for protein detection," *Analytical chemistry,* vol. 83, no. 23, pp. 9138-9145, 2011.
[43] S. Liebana and G. A. Drago, "Bioconjugation and stabilisation of biomolecules in biosensors," *Essays in biochemistry,* vol. 60, no. 1, pp. 59-68, 2016.
[44] J. F. Lutz, "Polymerization of oligo (ethylene glycol)(meth) acrylates: toward new generations of smart biocompatible materials," *Journal of Polymer Science Part A: Polymer Chemistry,* vol. 46, no. 11, pp. 3459-3470, 2008.
[45] N. M. Smeets, E. Bakaic, M. Patenaude, and T. Hoare, "Injectable and tunable poly (ethylene glycol) analogue hydrogels based on poly (oligoethylene glycol methacrylate)," *Chemical Communications,* vol. 50, no. 25, pp. 3306-3309, 2014.
[46] M. Patenaude, N. M. Smeets, and T. Hoare, "Designing Injectable, Covalently Cross-Linked Hydrogels for Biomedical Applications," *Macromolecular rapid communications,* vol. 35, no. 6, pp. 598-617, 2014.
[47] J.-F. Lutz and A. Hoth, "Preparation of ideal PEG analogues with a tunable thermosensitivity by controlled radical copolymerization of 2-(2-methoxyethoxy) ethyl methacrylate and oligo (ethylene glycol) methacrylate," *Macromolecules,* vol. 39, no. 2, pp. 893-896, 2006.
[48] E. Bakaic *et al.*, "Injectable and Degradable Poly (Oligoethylene glycol methacrylate) Hydrogels with Tunable Charge Densities as Adhesive Peptide-Free Cell Scaffolds," *ACS Biomaterials Science & Engineering,* vol. 4, no. 11, pp. 3713-3725, 2017.
[49] S. Sun and P. Wu, "On the thermally reversible dynamic hydration behavior of oligo (ethylene glycol) methacrylate-based polymers in water," *Macromolecules,* vol. 46, no. 1, pp. 236-246, 2012.
[50] N. M. Smeets, E. Bakaic, M. Patenaude, and T. Hoare, "Injectable poly (oligoethylene glycol methacrylate)-based hydrogels with tunable phase transition behaviours: Physicochemical and biological responses," *Acta biomaterialia,* vol. 10, no. 10, pp. 4143-4155, 2014.

[51] S. Ilican, Y. Caglar, and M. Caglar, "Preparation and characterization of ZnO thin films deposited by sol-gel spin coating method," *Journal of optoelectronics and advanced materials,* vol. 10, no. 10, pp. 2578-2583, 2008.

[52] S. Limem, D. McCallum, G. G. Wallace, and P. Calvert, "Inkjet printing of self-assembling polyelectrolyte hydrogels," *Soft Matter,* vol. 7, no. 8, pp. 3818-3826, 2011.

[53] P. S. Hume, C. N. Bowman, and K. S. Anseth, "Functionalized PEG hydrogels through reactive dip-coating for the formation of immunoactive barriers," *Biomaterials,* vol. 32, no. 26, pp. 6204-6212, 2011.

[54] X. Deng *et al.*, "Poly (oligoethylene glycol methacrylate) dip-coating: turning cellulose paper into a protein-repellent platform for biosensors," *Journal of the American Chemical Society,* vol. 136, no. 37, pp. 12852-12855, 2014.

[55] J. M. Asua, "Emulsion polymerization: from fundamental mechanisms to process developments," *Journal of Polymer Science Part A: Polymer Chemistry,* vol. 42, no. 5, pp. 1025-1041, 2004.

[56] B. Kriwet, E. Walter, and T. Kissel, "Synthesis of bioadhesive poly (acrylic acid) nano-and microparticles using an inverse emulsion polymerization method for the entrapment of hydrophilic drug candidates," *Journal of controlled release,* vol. 56, no. 1-3, pp. 149-158, 1998.

[57] I. Americas, *The HLB system: a time-saving guide to emulsifier selection*. ICI Americas, Incorporated, 1984.

[58] V. Kireev, Y. V. Sharshakova, V. Savel'yanov, and A. Klochkov, "Particle size distribution in suspension polymerisation of monomers dissolving their polymer," *International Polymer Science and Technology,* vol. 29, no. 12, pp. 27-29, 2002.

[59] V. Alvarado, X. Wang, and M. Moradi, "Stability proxies for water-in-oil emulsions and implications in aqueous-based enhanced oil recovery," *Energies,* vol. 4, no. 7, pp. 1058-1086, 2011.

[60] D.-W. Lim, K.-G. Song, K.-J. Yoon, and S.-W. Ko, "Synthesis of acrylic acid-based superabsorbent interpenetrated with sodium PVA sulfate using inverse-emulsion polymerization," *European Polymer Journal,* vol. 38, no. 3, pp. 579-586, 2002.

[61] D. Hunkeler, A. Hamielec, and W. Baade, "Mechanism, kinetics and modelling of the inverse-microsuspension homopolymerization of acrylamide," *Polymer,* vol. 30, no. 1, pp. 127-142, 1989.

[62] D. S. Tawfik and A. D. Griffiths, "Man-made cell-like compartments for molecular evolution," *Nature biotechnology,* vol. 16, no. 7, p. 652, 1998.

[63] M. Nakano, J. Komatsu, S.-i. Matsuura, K. Takashima, S. Katsura, and A. Mizuno, "Single-molecule PCR using water-in-oil emulsion," *Journal of biotechnology,* vol. 102, no. 2, pp. 117-124, 2003.

[64] A. Fire and S.-Q. Xu, "Rolling replication of short DNA circles," *Proceedings of the National Academy of Sciences,* vol. 92, no. 10, pp. 4641-4645, 1995.

[65] D. Liu, S. L. Daubendiek, M. A. Zillman, K. Ryan, and E. T. Kool, "Rolling circle DNA synthesis: small circular oligonucleotides as efficient templates for DNA polymerases," *Journal of the American Chemical Society,* vol. 118, no. 7, pp. 1587-1594, 1996.

[66] C. Carrasquilla, J. R. Little, Y. Li, and J. D. Brennan, "Patterned Paper Sensors Printed with Long-Chain DNA Aptamers," *Chemistry–A European Journal,* vol. 21, no. 20, pp. 7369-7373, 2015.

[67] M. J. Heller, "DNA microarray technology: devices, systems, and applications," *Annual review of biomedical engineering,* vol. 4, no. 1, pp. 129-153, 2002.
[68] A. Alsaafin and M. McKeague, "Functional nucleic acids as in vivo metabolite and ion biosensors," *Biosensors and Bioelectronics,* vol. 94, pp. 94-106, 2017.
[69] L. Farzin, M. Shamsipur, and S. Sheibani, "A review: Aptamer-based analytical strategies using the nanomaterials for environmental and human monitoring of toxic heavy metals," *Talanta,* vol. 174, pp. 619-627, 2017.
[70] J. H. Niazi, S. J. Lee, and M. B. Gu, "Single-stranded DNA aptamers specific for antibiotics tetracyclines," *Bioorganic & medicinal chemistry,* vol. 16, no. 15, pp. 7245-7253, 2008.
[71] C. L. Hamula, H. Zhang, F. Li, Z. Wang, X. C. Le, and X.-F. Li, "Selection and analytical applications of aptamers binding microbial pathogens," *TrAC Trends in Analytical Chemistry,* vol. 30, no. 10, pp. 1587-1597, 2011.
[72] D. Shangguan *et al.*, "Aptamers evolved from live cells as effective molecular probes for cancer study," *Proceedings of the National Academy of Sciences,* vol. 103, no. 32, pp. 11838-11843, 2006.
[73] P. F. Xiao *et al.*, "An improved gel-based DNA microarray method for detecting single nucleotide mismatch," *Electrophoresis,* vol. 27, no. 19, pp. 3904-3915, 2006.
[74] A. Y. Rubina *et al.*, "Hydrogel drop microchips with immobilized DNA: properties and methods for large-scale production," *Analytical biochemistry,* vol. 325, no. 1, pp. 92-106, 2004.
[75] J. Liu, "Oligonucleotide-functionalized hydrogels as stimuli responsive materials and biosensors," *Soft Matter,* vol. 7, no. 15, pp. 6757-6767, 2011.
[76] H. Cohen *et al.*, "Sustained delivery and expression of DNA encapsulated in polymeric nanoparticles," *Gene therapy,* vol. 7, no. 22, p. 1896, 2000.
[77] Q. Garrett, R. C. Chatelier, H. J. Griesser, and B. K. Milthorpe, "Effect of charged groups on the adsorption and penetration of proteins onto and into carboxymethylated poly (HEMA) hydrogels," *Biomaterials,* vol. 19, no. 23, pp. 2175-2186, 1998.
[78] G. Klöck *et al.*, "Biocompatibility of mannuronic acid-rich alginates," *Biomaterials,* vol. 18, no. 10, pp. 707-713, 1997.
[79] V. Barsky, A. Kolchinsky, Y. P. Lysov, and A. Mirzabekov, "Biological microchips with hydrogel-immobilized nucleic acids, proteins, and other compounds: properties and applications in genomics," *Molecular Biology,* vol. 36, no. 4, pp. 437-455, 2002.
[80] A. Relógio, C. Schwager, A. Richter, W. Ansorge, and J. Valcárcel, "Optimization of oligonucleotide-based DNA microarrays," *Nucleic acids research,* vol. 30, no. 11, pp. e51-e51, 2002.
[81] B. E. Rapp, *Microfluidics: Modeling, Mechanics and Mathematics*. William Andrew, 2016.
[82] J. Meinkoth and G. Wahl, "Hybridization of nucleic acids immobilized on solid supports," *Analytical biochemistry,* vol. 138, no. 2, pp. 267-284, 1984.
[83] T. Brown, "Hybridization analysis of DNA blots," *Current protocols in immunology,* vol. 6, no. 1, pp. 10.6. 13-10.6. 27, 1993.
[84] G. H. Keller and M. M. Manak, *DNA probes*. Macmillan Publishers Ltd, 1989.
[85] T. Han *et al.*, "Improvement in the reproducibility and accuracy of DNA microarray quantification by optimizing hybridization conditions," in *BMC bioinformatics*, 2006, vol. 7, no. 2: BioMed Central, p. S17.

[86] S. M. Solberg and C. C. Landry, "Adsorption of DNA into mesoporous silica," *The Journal of Physical Chemistry B,* vol. 110, no. 31, pp. 15261-15268, 2006.
[87] A. Rentmeister, A. Bill, T. Wahle, J. Walter, and M. Famulok, "RNA aptamers selectively modulate protein recruitment to the cytoplasmic domain of β-secretase BACE1 in vitro," *Rna,* vol. 12, no. 9, pp. 1650-1660, 2006.
[88] N. Li, H. H. Nguyen, M. Byrom, and A. D. Ellington, "Inhibition of cell proliferation by an anti-EGFR aptamer," *PloS one,* vol. 6, no. 6, p. e20299, 2011.
[89] N. Savory *et al.*, "In silico maturation of binding-specificity of DNA aptamers against Proteus mirabilis," *Biotechnology and bioengineering,* vol. 110, no. 10, pp. 2573-2580, 2013.
[90] H. Schaller, C. Nüsslein, F. J. Bonhoeffer, C. Kurz, and I. Nietzschmann, "Affinity Chromatography of DNA-Binding Enzymes on Single-Stranded DNA-Agarose Columns," *European journal of biochemistry,* vol. 26, no. 4, pp. 474-481, 1972.
[91] T. S. Romig, C. Bell, and D. W. Drolet, "Aptamer affinity chromatography:: combinatorial chemistry applied to protein purification," *Journal of Chromatography B: Biomedical Sciences and Applications,* vol. 731, no. 2, pp. 275-284, 1999.
[92] Y. Koh *et al.*, "Bead affinity chromatography in a temperature-controllable microsystem for biomarker detection," *Analytical and bioanalytical chemistry,* vol. 404, no. 8, pp. 2267-2275, 2012.
[93] S. Cho, S. H. Lee, W. J. Chung, Y. K. Kim, Y. S. Lee, and B. G. Kim, "Microbead-based affinity chromatography chip using RNA aptamer modified with photocleavable linker," *Electrophoresis,* vol. 25, no. 21-22, pp. 3730-3739, 2004.
[94] G. D. Huy, N. Jin, B.-C. Yin, and B.-C. Ye, "A novel separation and enrichment method of 17β-estradiol using aptamer-anchored microbeads," *Bioprocess and biosystems engineering,* vol. 34, no. 2, pp. 189-195, 2011.
[95] Y. Hoshino *et al.*, "Preparation of nanogel-immobilized porous gel beads for affinity separation of proteins: fusion of nano and micro gel materials," *Polymer Journal,* vol. 47, no. 2, p. 220, 2015.
[96] A. Anisa and A. H. Nour, "Affect of Viscosity and Droplet Diameter on water-in-oil (w/o) Emulsions: An Experimental Study," *World Academy of Science, Engineering and Technology,* vol. 62, 2010.
[97] K. van Dijke, I. Kobayashi, K. Schroën, K. Uemura, M. Nakajima, and R. Boom, "Effect of viscosities of dispersed and continuous phases in microchannel oil-in-water emulsification," *Microfluidics and nanofluidics,* vol. 9, no. 1, pp. 77-85, 2010.
[98] P. Kent and B. R. Saunders, "The role of added electrolyte in the stabilization of inverse emulsions," *Journal of colloid and interface science,* vol. 242, no. 2, pp. 437-442, 2001.
[99] M. P. Aronson and M. F. Petko, "Highly concentrated water-in-oil emulsions: Influence of electrolyte on their properties and stability," *Journal of Colloid and Interface Science,* vol. 159, no. 1, pp. 134-149, 1993.
[100] V. Kurenkov, T. Osipova, E. Kuznetsov, and V. Myagchenkov, "Polymerization of acrylamide using potassium persulfate as initiator," *Vysokomol. Soedin. Seriya B,* vol. 20, pp. 647-650, 1978.
[101] L.-W. Chen, B.-Z. Yang, and M.-L. Wu, "Synthesis and kinetics of microgel in inverse emulsion polymerization of acrylamide," *Progress in organic coatings,* vol. 31, no. 4, pp. 393-399, 1997.

Appendix A: Supplementary Figures

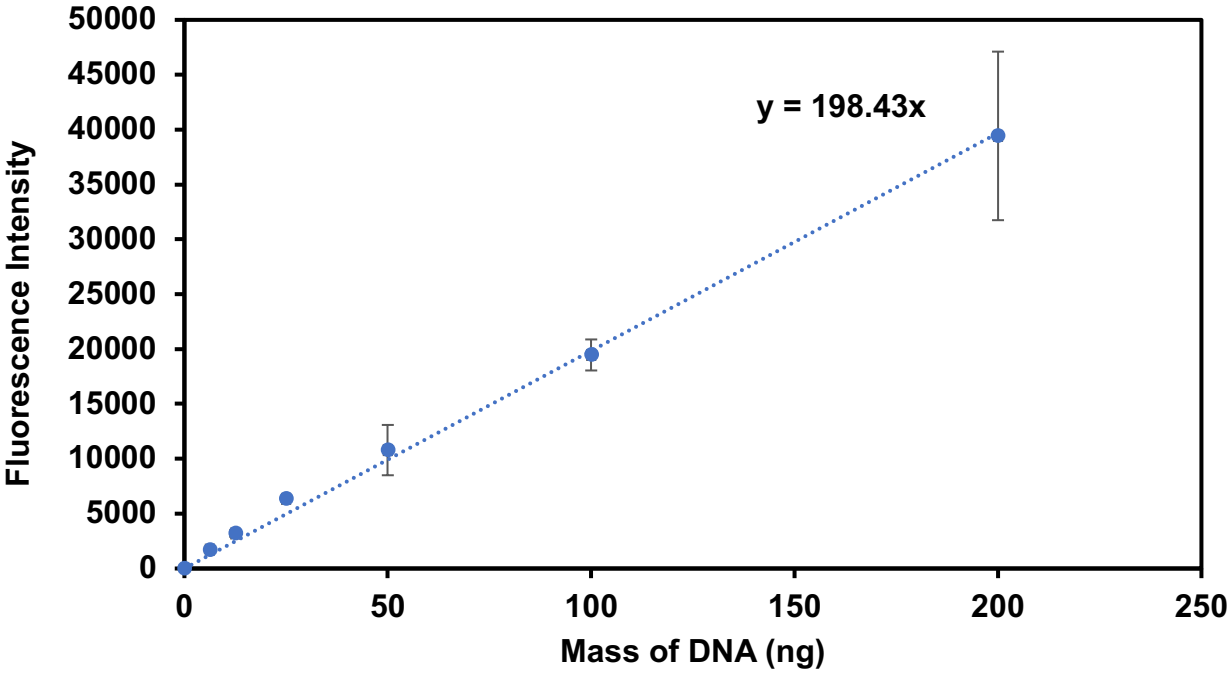

Figure A.1. High concentration Quantifluor® ssDNA standard curve.

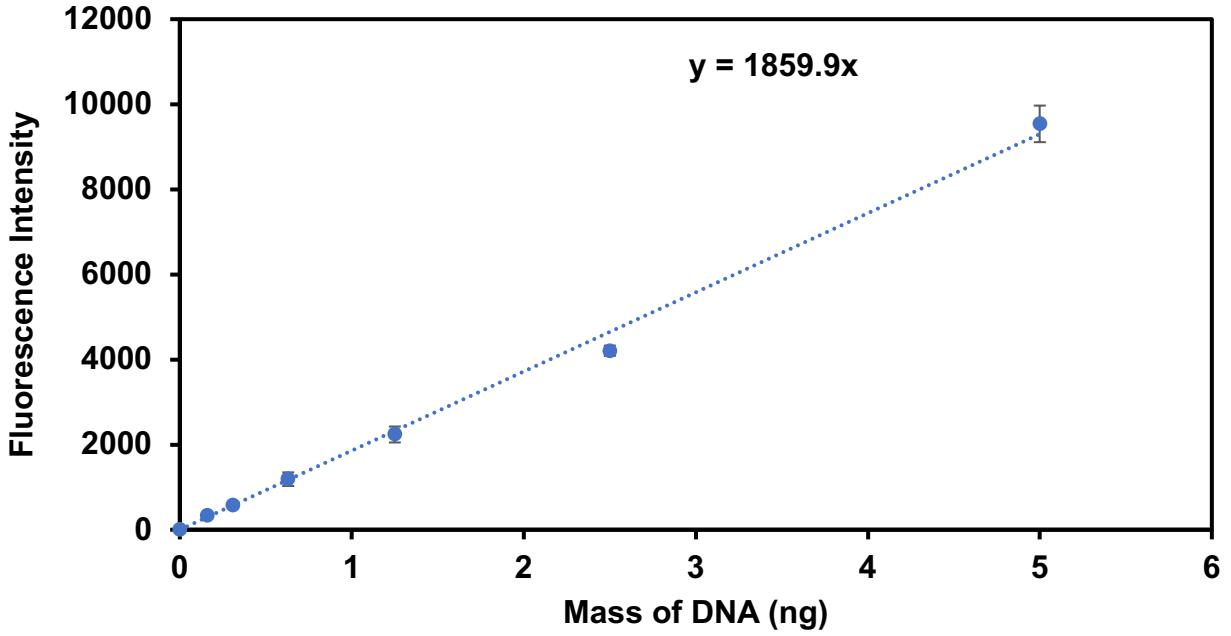

Figure A.2 Low concentration Quantifluor® ssDNA standard curve.

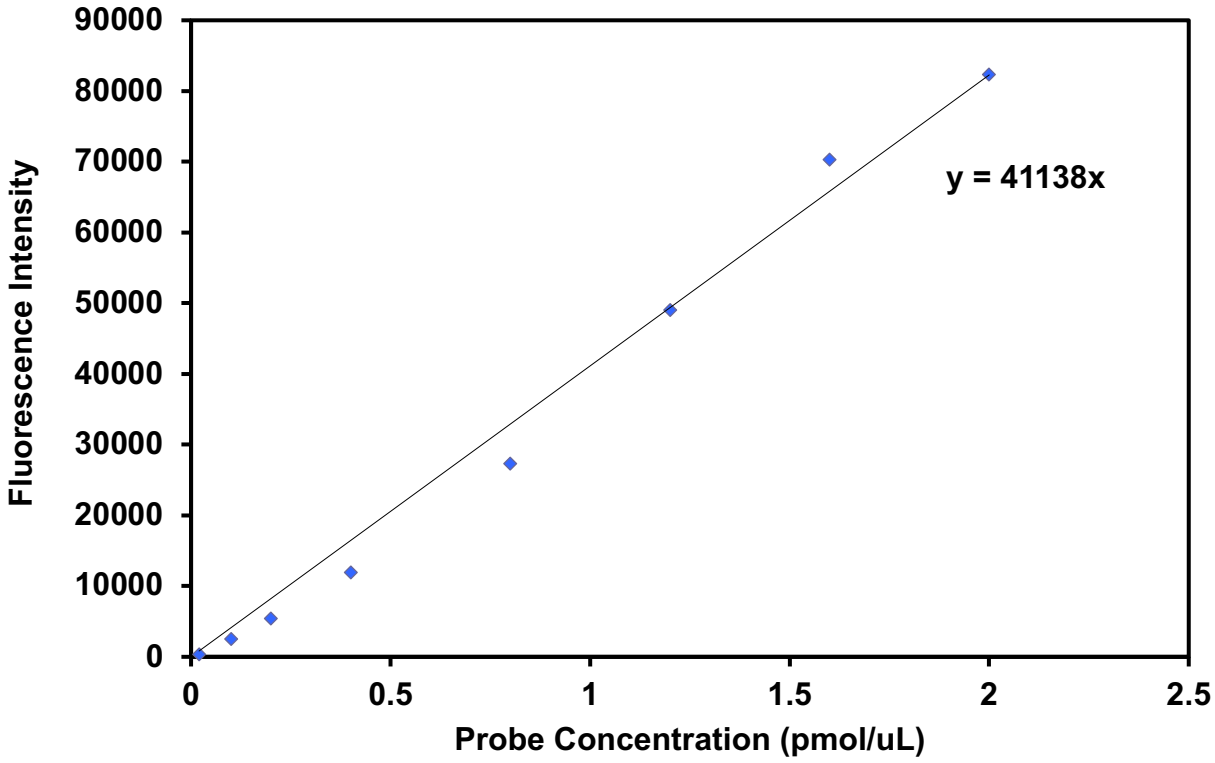

Figure A.3 Fluorescent probe standard curve.